

# Syn-collisional magmatic record of Indian steep subduction by 50 Ma

Yue Qi<sup>1,2,3</sup>, Chris J. Hawkesworth<sup>3</sup>, Qiang Wang<sup>1,2,4,†</sup>, Derek A. Wyman<sup>5</sup>, Zheng-Xiang Li<sup>6</sup>, Han Dong<sup>7</sup>, Tao Ma<sup>7</sup>, Fukun Chen<sup>8</sup>, Wan-Long Hu<sup>1,2</sup>, and Xiu-Zheng Zhang<sup>1</sup>

<sup>1</sup>State Key Laboratory of Isotope Geochemistry, Guangzhou Institute of Geochemistry, Chinese Academy of Sciences, Guangzhou 510640, China

<sup>2</sup>College of Earth and Planetary Sciences, University of Chinese Academy of Sciences 100049, China

<sup>3</sup>School of Earth Sciences, University of Bristol, Wills Memorial Building, Queens Road, Bristol BS8 1RJ, UK

<sup>4</sup>Chinese Academy of Sciences Center for Excellence in Tibetan Plateau Earth Sciences, Beijing 100101, China

<sup>5</sup>School of Geosciences, University of Sydney, Sydney, New South Wales 2006, Australia

<sup>6</sup>Earth Dynamics Research Group, The Institute for Geoscience Research (TIGeR), School of Earth and Planetary Sciences, Curtin University, Perth, Western Australia 6845, Australia

<sup>7</sup>The Third Geological and Mineral Resource Survey Institute of Geology and Mineral Bureau of Gansu Province, Lanzhou 730050, China

<sup>8</sup>Key Laboratory of Crust-Mantle Materials and Environments, School of Earth and Space Sciences, University of Science and Technology of China, Hefei 230026, China

## ABSTRACT

Subduction of Indian continental lithosphere during the Asia-India collision played an important role in the formation and evolution of the Himalaya-Tibetan orogen. However, the geometry of early Indian continental subduction remains debated. Given that the Indian continent is characterized by enriched isotope ratios ( $^{87}\text{Sr}/^{86}\text{Sr} > 0.730$ ,  $\epsilon_{\text{Nd}}(t) < -10$ ), relative to those in subducted oceanic materials ( $^{87}\text{Sr}/^{86}\text{Sr} < 0.704$ ,  $\epsilon_{\text{Nd}}(t) \approx +8$ ), changes in the composition of magmatic rocks with time, in particular their radiogenic isotope ratios, is used to constrain the timing and nature of continental subduction. This study reports the field relations, zircon U-Pb ages and geochemical composition of a syn-collisional batholith that crosscuts the central Indus-Yarlung Zangbu suture in the Saga area of southern Tibet. Zircon U/Pb ages for the batholith mainly range from 50 to 46 Ma. Samples from the Lopu Range batholith have enriched zircon Hf ( $\epsilon_{\text{Hf}}(t) = -0.4$  to  $-8.6$ ) and whole rock  $^{87}\text{Sr}/^{86}\text{Sr}_i = 0.7094\text{--}0.7121$  and  $\epsilon_{\text{Nd}}(t) = -7.3$  to  $-9.8$ , suggesting that they were derived from a mixture of juvenile Gangdese and isotopically enriched Indian crustal materials. This result indicates that subduction of Indian crustal rocks occurred before 50 Ma in the central Himalaya. The geochemical composition and distribution of high volume ca. 51 Ma magmatism in the

Gangdese belt, combined with thermal models of the subduction zone, suggests a steepening of the subducted Indian continental lithosphere occurred between the onset of India-Asia collision (59 Ma) and 46 Ma in the central-eastern Himalaya.

## INTRODUCTION

The convergence of India and Asia, accompanied by Indian continental subduction, has resulted in the largest and highest recent orogen: the Himalaya-Tibetan orogenic system (e.g., Dewey and Bird, 1970; Dewey, 1988; Allègre et al., 1984; Hodges, 2000; Yin and Harrison, 2000; Li et al., 2015). The current state of underthrusting of the Indian continental lithosphere beneath the Asian lithosphere is well documented in seismic images, which show spatial variations from west to east along the suture (e.g., Nelson et al., 1996; Li et al., 2008; Nábělek et al., 2009; Zhao et al., 2010; Chen et al., 2015; Li and Song, 2018). In the west, flat lying Indian lithosphere reaches the southern margin of the Tarim basin, and subducted Indian crust only reaches depths of ~90 km (Van der Voo et al., 1999; Li et al., 2008; Zhao et al., 2010; Li and Song, 2018). At longitude 85°E, the flat-lying Indian lithosphere extends to the Bangong-Nujiang suture (Van der Voo et al., 1999; Tilmann et al., 2003; Nábělek et al., 2009; Zhao et al., 2010; Shi et al., 2015; Li and Song, 2018), whereas at 90°E longitude the Indian lithosphere appears to have been subducted vertically beneath the Indus-Yar-

lung Zangbu suture (IYZS; Li et al., 2008; Shi et al., 2015, 2016; Chen et al., 2015; Li and Song, 2018). However, the present geometric structure of the subducted Indian lithosphere does not reflect its initial state at the onset of India-Asia collision. In the western Himalaya, the ultra-high pressure (UHP) complexes, exposed in the Kaghan and Tso Moriri areas, equilibrated at depths of 145–160 km at ca. 50 Ma (de Sigoyer et al., 2000, 2004; Guillot et al., 2008; Wilke et al., 2015), and they are thought to have resulted from early steep continental subduction before 51 Ma (Leech et al., 2005; Guillot et al., 2008; Donaldson et al., 2013). In the central Himalaya, collision-related high-pressure (HP) metamorphic complexes in the Lopu range area imply steep India continental subduction began after the India-Asia collision and continued until ca. 38 Ma (Laskowski et al., 2016, 2017). The HP complexes in the Garhwal area indicate relatively shallow (flat) subduction before 50 Ma in the eastern Himalaya (Guillot et al., 2008).

The focus here is to reconstruct the initial geometry of Indian continental subduction from changes in the composition of magmatic rocks. The initial India-Asia collision took place by ca. 59 Ma in the central-eastern Himalaya and by 54 Ma in the western Himalaya (from the age of Asia-derived materials deposited on the Indian plate, DeCelles et al., 2014; Wu et al., 2014; Hu et al., 2015, 2016; Najman et al., 2017). The subsequent subduction of the Indian continent initiated UHP-HP metamorphism, and resulted in a change in the source materials for igneous rocks from

<sup>†</sup>Corresponding author: wqiang@gig.ac.cn.

Asia-dominated to India-dominated along the continental margin. The northern edge of the Indian continent (the Tethyan Himalaya) consists predominantly of mature crustal materials with radiogenic isotope compositions ( $^{87}\text{Sr}/^{86}\text{Sr} > 0.730$ ,  $\epsilon_{\text{Nd}}(t) < -10$ , Ahmad et al., 2000; Richards et al., 2005) that are enriched relative to those in subducted oceanic material ( $^{87}\text{Sr}/^{86}\text{Sr} < 0.704$ ,  $\epsilon_{\text{Nd}}(t) \approx +8$ , e.g., Miller et al., 2003). When crustal materials are subducted to subarc depths (80–160 km), fluids and/or melts enriched in incompatible elements are released from the subducted crust and transferred into the overlying mantle wedge (Mahéo et al., 2009; Hermann et al., 2013; Zheng and Chen, 2016). Shallow subduction would transport enriched materials far from the suture zone area in contrast to steep subduction that delivers enriched materials only to area relatively near the suture zone. Thus, changes in the composition of magmatic rocks with time in southern Lhasa especially in their radiogenic isotope ratios, may further constrain the onset and style of continental subduction. In the Lhasa terrane, a ca. 51 Ma relatively high volume magmatic event occurred during Indian continental subduction (Zhu et al., 2019, and references therein), providing an excellent opportunity to constrain the geometry of early Indian continental subduction.

In this study we constrain the age of early Indian continent subduction in the central Himalaya by establishing the crystallization age of a syn-collisional batholith in the Lopu Range area that crosscuts the suture zone, and examine the style and geometry of subduction by tracing the changes in the isotope ratios of the igneous rocks in the region. The field relations indicate that the Lopu Range batholith was emplaced into the Indus-Yarlung Zangbu suture that is the tectonic boundary between India and Asia after the major deformation associated with collision. The zircon U-Pb ages and geochemical composition of the Lopu Range batholith highlight that subduction of the Indian continent in the central Himalaya took place before 50 Ma. This is consistent with the ages of collision-related metamorphism in the Himalaya, suggesting that magmatism can be used to constrain the onset of continental subduction. Integrating numerical models of the thermal evolution, and the geochemical composition and location of the ca. 51 Ma high volume magmatic event in the eastern Gangdese belt, we argue that steep subduction of the Indian continental plate continued to at least 46 Ma after the onset of India-Asia collision (59 Ma) in the central-eastern Himalaya.

## GEOLOGICAL SETTING AND THE SAMPLES ANALYZED


### Regional Setting

The Indus-Yarlung Zangbu suture (IYZS) contains remnants of Neo-Tethyan oceanic lithosphere, it separates India to the south from Asia to the north (Chang and Zheng, 1973; Allègre et al., 1984; Dewey, 1988; Yin and Harrison, 2000), and it consists of ophiolite massifs, an ophiolitic mélange, and subduction-accretion mélanges (Dai et al., 2012, 2013; Hébert et al., 2012 and references therein). The ophiolite massifs formed at 177–150 Ma and 130–88 Ma and they were accreted onto the southern margin of Lhasa prior to the India-Asia collision (Guillemette et al., 2009, 2012; Hébert et al., 2012; Dai et al., 2013). The ophiolitic mélange occurs to the south of the ophiolite massifs and it consists of deformed and metamorphosed, foliated amphibolite blocks derived from reworking of the ophiolites (Dai et al., 2012; Hébert et al., 2012). The subduction-accretion mélanges have a Late Triassic to Early Cretaceous matrix with Permian to Cretaceous meter-to-kilometer scale blocks that include marine limestone, sandstone, chert, basalt, metabasite, and shale (Searle et al., 1987; Zhu et al., 2005; Cai et al., 2012; An et al., 2017; Metcalf and Kapp, 2017, 2019; Wang et al., 2017a, 2018). These subduction-accretion mélanges are thought to have formed in an oceanic subduction zone beneath the ophiolite belts (Searle et al., 1987; Cai et al., 2012; Metcalf and Kapp, 2017, 2019; Wang et al., 2017a, 2018).

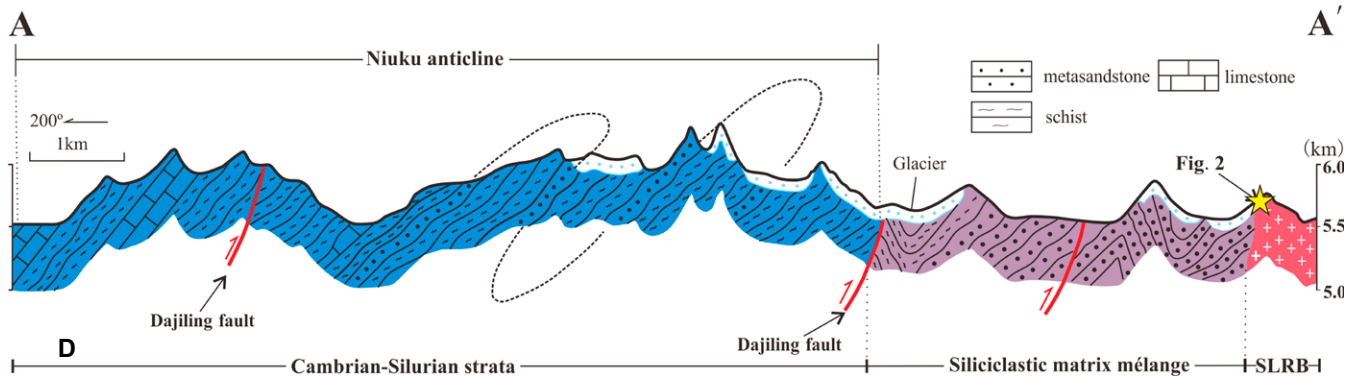
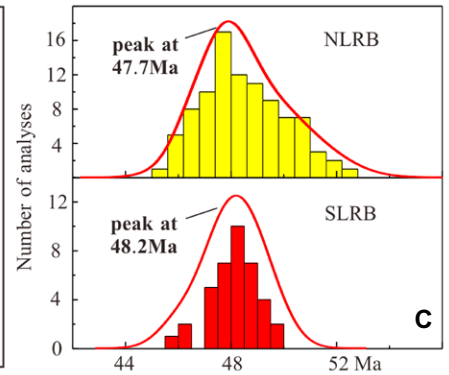
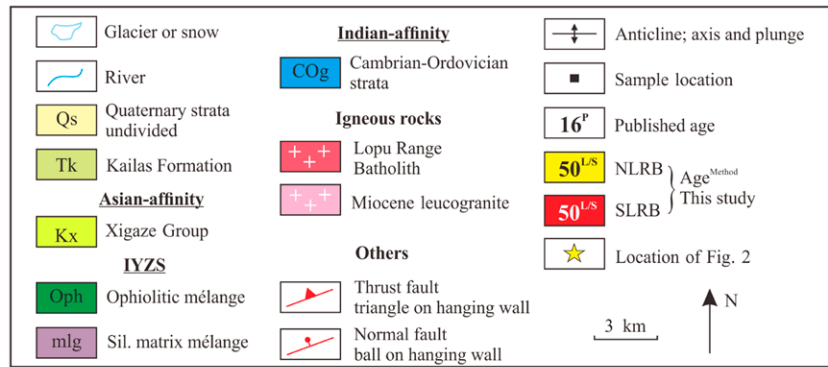
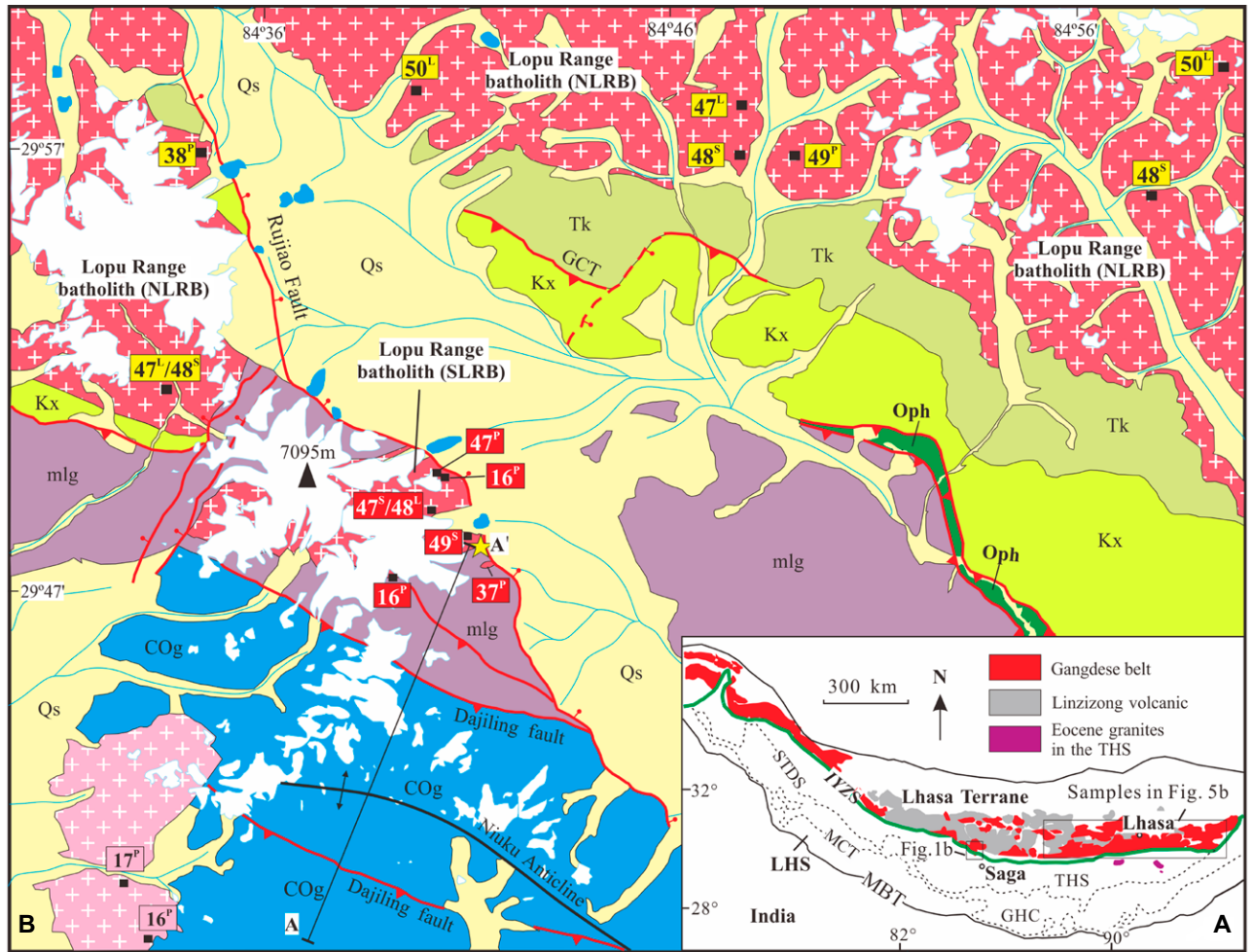
North of the IYZS, the Lhasa Terrane, as the southern margin of the Asian continent, can be subdivided into the northern, central, and southern terranes, characterized by ancient crust in the center and Mesozoic juvenile crust accreted along both its northern and southern margins (Zhu et al., 2011, 2013; Hou et al., 2015; Zhou et al., 2017). The Gangdese magmatic belt in the southern Lhasa Terrane is dominated by the Cretaceous–Tertiary Gangdese Batholith and the Paleocene–early Eocene Linzizong volcanic succession (Fig. 1A, Allègre et al., 1984; Debon et al., 1987; Chung et al., 2005; Chu et al., 2011; Zhu et al., 2011, 2019). The Linzizong volcanic succession ranges from basalt to rhyolite and it can be divided into three formations: the Dianzhong (60–58 Ma), Nianbo (55–52 Ma), and Pana formations (52–49 Ma, Zhu et al., 2015, 2019; Liu et al., 2018). The Jurassic to early Eocene components of the Gangdese belt have relatively depleted Sr-Hf-Nd isotope ratios, indicating sources associated with the subduction of the Neo-Tethyan oceanic lithosphere (Chung et al., 2005; Chu et al., 2011; Zhu et al., 2019 and references therein). Some studies (e.g., Hou

et al., 2015; Wang et al., 2015) also proposed that the magmatic rocks from the western Gangdese belt have lower  $\epsilon_{\text{Hf}}$  values than those in the eastern Gangdese belt, suggesting that there was some ancient basement beneath the western Gangdese belt. To the south of the Gangdese arc, the Xigaze forearc basin consists of Cretaceous to lower Eocene clastic units that were mainly derived from the Gangdese arc (Wu et al., 2010; Orme et al., 2015; Orme and Laskowski, 2016; Wang et al., 2017b). South of the IYZS, the Tethyan Himalaya Sequence (THS) represents the deformed remnant of the northern continental margin of the Indian subcontinent, which mainly consists of Cambrian–Eocene sandstone, mudstones, shales, and limestones (Liu and Einsele, 1994; Ding et al., 2005; Zhu et al., 2013).

The study area is located northwest of Saga County, where the Lopu range (or Lopukangri) with an elevation up to 7095 m includes the main peak of the Gangdese mountains in southern Tibet (Fig. 1). Extending to ~50 km south of the Lopu range, the Sangdanlin section preserves the typical stratigraphic record after the India-Asia collision, in which hypermature quartzose sandstones sourced from India are progressively replaced upward by immature volcanic-plutonic clastic sandstones derived from Asia (Ding et al., 2005; DeCelles et al., 2014; Wu et al., 2014;



**Figure 1.** A geological map of south Tibet showing the tectonic terranes and the location of the Lopu Range batholith. (A) Simplified geological map of southern Tibet. (B) Simplified geologic map of the Lopu Range area based on our 1:50,000 geological mapping and the maps of Laskowski et al. (2017) and Metcalf and Kapp (2017). (C) Histogram of zircon U-Pb ages of the Lopu Range batholith, showing data from outcrops north and south of the IYSZ separately for comparison. The red line is the probability density curve. (D) The cross-section A–A' in Figure 1B, original field information is shown in Figure S1 (see footnote 1). In Figure 1B, 50<sup>L</sup>/48<sup>S</sup> show zircon U-Pb ages determined using both laser ablation-inductively coupled plasma-mass spectrometry (<sup>L</sup>) and secondary ion mass spectrometry (<sup>S</sup>) methods. IYZS—Indus-Yarlung Zangbu suture; STDS—South Tibetan Detachment System; MCT—Main Central Thrust; MBT—Main Boundary Thrust; THS—Tethyan Himalaya Sedimentary Sequences; GHC—Greater Himalayan Crystalline Complex; LHS—Lesser Himalayan Series; NLRB—the Lopu Range batholith north of the IYZS; SLRB—the Lopu Range batholith south of the IYZS; Sil.—siliciclastic.



Hu et al., 2015, 2016). The radiolarian and nanofossil biostratigraphy, and the detrital zircon ages, indicate that the Asia-derived detritus was first deposited on the distal edge of India at ca. 59 Ma in the central Himalaya (DeCelles et al., 2014; Hu et al., 2015).

### Geology of the Lopu Area

The Lopu Range area spans the IYZS, and it comprises a number of lithotectonic units including, from north to south: (1) the Gangdese arc belt, (2) Oligocene–Miocene Kailas Formation, (3) Xigaze fore-arc basin strata, (4) IYZS mélangé, and (5) Tethyan Himalaya sedimentary Sequence (THS) (Fig. 1B). The granitoids in this area are post tectonic, they extend across the IYZS and are referred to here as the Lopu Range batholith (LRB).

The LRB north of the IYZS (NLRB) consists mostly of medium to fine grained quartz monzonites and granites. Published zircon U–Pb ages indicate that these granitoids were emplaced at 49 Ma and 38 Ma (Laskowski et al., 2017). The quartz monzonites are composed of plagioclase (30–35 vol%), potassium-feldspar (35–30 vol%), quartz (25–20 vol%), biotite (5 vol%), and amphibole (~2 vol%), and the granites contain potassium-feldspar (~40 vol%), plagioclase (30–35 vol%), quartz (~25 vol%), and minor biotite (~2 vol%). The Oligocene–Miocene Kailas Formation (Tk) consists of interbedded cobble gravel pebble conglomerate, sandstone, and minor volcanic tuffs, and it forms a buttress unconformity on the NLRB. To the south, the south dipping Great Counter Thrust puts the Xigaze fore-arc basin strata in the hanging wall and the Oligocene–Miocene Kailas Formation in the footwall (Ding et al., 2005; Sanchez et al., 2013; Orme et al., 2015, Laskowski et al., 2017, Fig. 1B). In the Lopu area the Xigaze Group consists of a >4.5 km shoaling upward sequence of sandstone, conglomerate, and sandy limestone (Wu et al., 2010; Orme et al., 2015).

The IYZS in the Lopu Range area is represented by ophiolitic mélangé (Oph) in fault contact with the Xigaze fore-arc sequence, and a unit of greenschist facies siliciclastic matrix mélangé (mlg) that is in fault contact with the ophiolitic mélangé (Metcalf and Kapp, 2017) (Fig. 1B). The siliciclastic matrix mélangé consists of decimeter to kilometer blocks in a shale matrix with occasional sandstone, and it was built on the southern margin of Asia during Neo-Tethyan oceanic subduction (Metcalf and Kapp, 2017). Further south, the THS strata consist of muscovite-quartz schists, limestone, quartzite, and phyllite, which typically underwent greenschist amphibolite facies metamorphism, forming the core of the Niuku anticline (Ding et al., 2005;

Laskowski et al., 2017; Fig. 1B). Detrital zircon ages from these strata yield maximum depositional ages between 535 and 437 Ma, indicating that this unit consists of Cambrian–Silurian strata (COg, Laskowski et al., 2017). Our field mapping showed that the Dajiling fault juxtaposes THS strata in the hanging wall against siliciclastic matrix mélangé in the footwall on the north limb of the Niuku anticline (Figs. 1B and 1D; Fig. S1<sup>1</sup>). The south limb of the Niuku anticline lies beyond our mapping area, but a previous study suggested that the Dajiling fault to the south dips south and juxtaposes Tethyan phyllite in the hanging wall against footwall paragneiss, quartzite, and schist (Laskowski et al., 2017). According to the ages of undeformed leucogranite that intrudes into the core of the Niuku anticline, the timing of deformation within the THS in the Lopu Range area occurred prior to ca. 45 Ma (Ding et al., 2005). Our 1:5000 scale, 20 km geological cross-section (A–A' in Fig. 1D and detailed in Fig. S1) was constructed across siliciclastic matrix mélangé and THS strata that form the core of the Niuku anticline.

The LRB south of the IYZS (SLRB) is mostly covered by glaciers, and the outcrops predominantly consist of medium-fine grained quartz monzonite (Figs. 1B, 2A, and 2B), similar to the main phase of the NLRB. Laskowski et al. (2017) reported that the contact between the SLRB and siliciclastic matrix mélangé was intrusive along the northern boundary and partially faulted along the southern boundary. We mapped a contact metamorphic aureole (Figs. 2C–2E) and metapelite enclaves within the intrusion (Fig. 2F) along the southern contact boundary between SLRB and siliciclastic matrix mélangé. The contact hornfels contains quartz, muscovite, biotite and occasionally with andalusite porphyroblasts, and it is either massive (Fig. 2E) or with a slight lamination due to mimetic orientation of the mica (Fig. 2D). There is therefore an intrusive relationship between the SLRB and its country rocks. Some Neogene (ca. 16 Ma) two-mica leucogranite dikes intrude the SLRB, the siliciclastic matrix mélangé and THS strata (Fig. S1, Ding et al., 2005; Laskowski et al., 2017).

### ANALYTICAL RESULTS

Twenty-one samples were collected, nineteen from NLRB and two from SLRB. The analytical methods, the sample locations, the zircon U–Pb

<sup>1</sup>Supplemental Material. Analytical methods, field geological cross-section, and analytical results for the Lopu Range batholith from southern Tibet. Please visit <https://doi.org/10.1130/GSAB.S.12746846> to access the supplemental material, and contact editing@geosociety.org with any questions.

ages and Hf isotope compositions, and whole rock geochemical and Sr–Nd isotope ratios are presented in the Supplemental Material (Tables S1 and S2; see footnote 1).

### Zircon U–Pb Ages and Hf Isotope Compositions

Six samples from the NLRB and two samples from the SLRB were selected for zircon U–Pb dating. The zircons in these samples are euhedral and characterized by oscillatory zoning, with length-width ratios from 1:1–1:3 (Fig. 3). No inherited zircon grains were observed. Five samples of quartz monzonites from the NLRB yielded <sup>206</sup>Pb/<sup>238</sup>U zircon ages of 47.9 ± 0.5 Ma, 47.3 ± 0.4 Ma/47.8 ± 0.7 Ma (laser ablation–inductively coupled plasma–mass spectrometry/secondary ion mass spectrometry/[L/S]), 49.6 ± 0.6 Ma, 48.4 ± 0.5 Ma, and 50.3 ± 0.5 Ma (Figs. 4A–4F). One granite sample from the NLRB yielded slightly younger <sup>206</sup>Pb/<sup>238</sup>U ages of 46.6 ± 0.4 Ma (Fig. 4G). The two quartz monzonite samples from the SLRB yielded <sup>206</sup>Pb/<sup>238</sup>U zircon ages of 47.2 ± 0.7 Ma/48.1 ± 0.4 Ma (L/S) and 48.8 ± 0.5 Ma (Figs. 4H–4J), and these ages are similar to those of quartz monzonites from the NLRB (Fig. 1C). Hf isotope ratios were determined on all of the dated zircon grains. Zircons from the NLRB have negative  $\epsilon_{\text{Hf}}(t)$  values (–0.4 to –8.6), similar to those (–1.1 to –7.7) of zircons from the SLRB (Fig. 5).

### Whole Rock Geochemical and Sr–Nd Isotopic Compositions

In the NLRB, the quartz monzonite samples, have SiO<sub>2</sub> (64.4–68.6 wt%), A/CNK (Al<sub>2</sub>O<sub>3</sub>/(CaO + Na<sub>2</sub>O + K<sub>2</sub>O) = 0.86–0.94), and MgO (1.57–2.23 wt%) values (Table S2) that are magnesian calc-alkalic to alkali-calcic (Fig. 6). The granite samples from the NLRB have higher SiO<sub>2</sub> (72.6–75.7 wt%), A/CNK (0.91–1.13), and lower MgO (0.22–1.12 wt%) (Table S2), and they are magnesian calc-alkalic to ferroan alkali-calcic (Fig. 6). The quartz monzonites from the SLRB have SiO<sub>2</sub> (64.3–64.9 wt%), A/CNK (0.88–0.90), and MgO (2.00–2.16 wt%) (Table S2), similar to those in the NLRB (Fig. 6). All samples are K-rich (K<sub>2</sub>O/Na<sub>2</sub>O = 1.31–1.92), with negative correlations between SiO<sub>2</sub> and MgO, CaO, TiO<sub>2</sub>, and P<sub>2</sub>O<sub>5</sub> contents (Figs. S2B–S2E; see footnote 1), and significant positive correlations between SiO<sub>2</sub> and A/CNK and K<sub>2</sub>O + Na<sub>2</sub>O (Figs. S2A and S2F).

The quartz monzonite samples from the NLRB have restricted (La/Yb)<sub>N</sub> ratios of 15.7–28.8, in contrast to the larger variation (7.5–77.6) in the granite (Table S2). The quartz monzonite samples from the SLRB have similar (La/Yb)<sub>N</sub> ratios

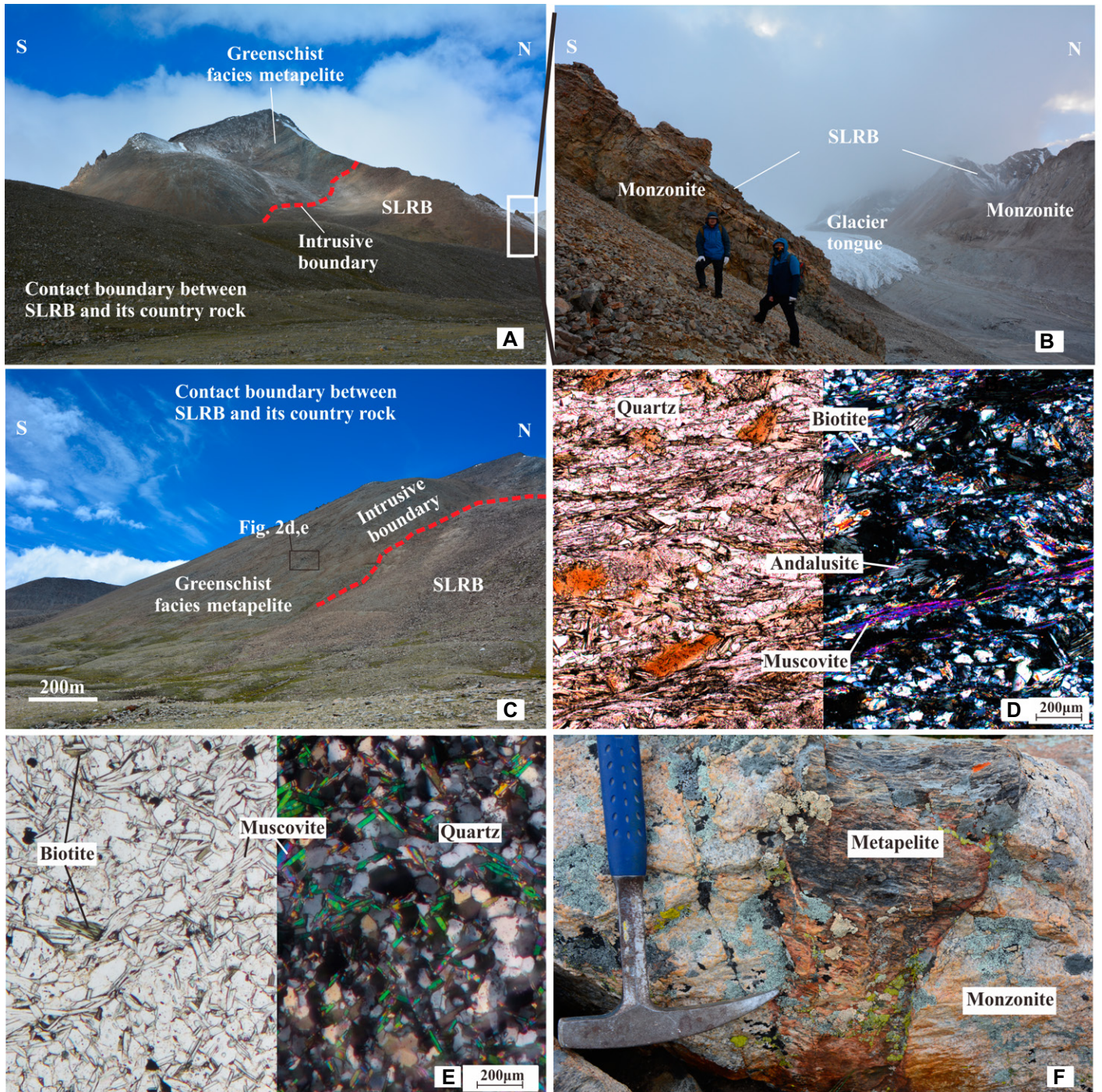


**Figure 2.** (A–C) Photographs of selected outcrops of the Lopu Range (Tibet) batholith (south) and its country rock (greenschist facies metapelite); (D and E) photomicrograph of the andalusite-bearing mica schist and two mica hornfels in plane polarized (left) and crossed polars (right) light, respectively. (F) A metapelite enclave in the Lopu Range batholith (south). SLRB—the Lopu Range batholith south of the IYZS.

(22.5–23.5) to those in the NLRB (Table S2). All rocks have low  $(Gd/Yb)_N$  ratios (0.9–2.7), negative Eu anomalies ( $Eu/Eu^* = 0.28–0.65$ ), and variable Sr/Y ratios (3.3–30.9) (Table S2). They have relatively flat heavy rare earth element

patterns (Fig. 7A), and they are enriched in large ion-lithophile elements relative to the high field strength elements (Fig. 7B). The Zr saturation temperatures calculated from whole rock compositions vary from 678 to 746 °C (Table S2).

Samples with  $^{87}Rb/^{86}Sr > 10$  were omitted from the discussion of the Sr isotope ratios simply because it causes a large uncertainty in the calculated initial Sr ratios (Wu et al., 2002). The rocks in the NLRB

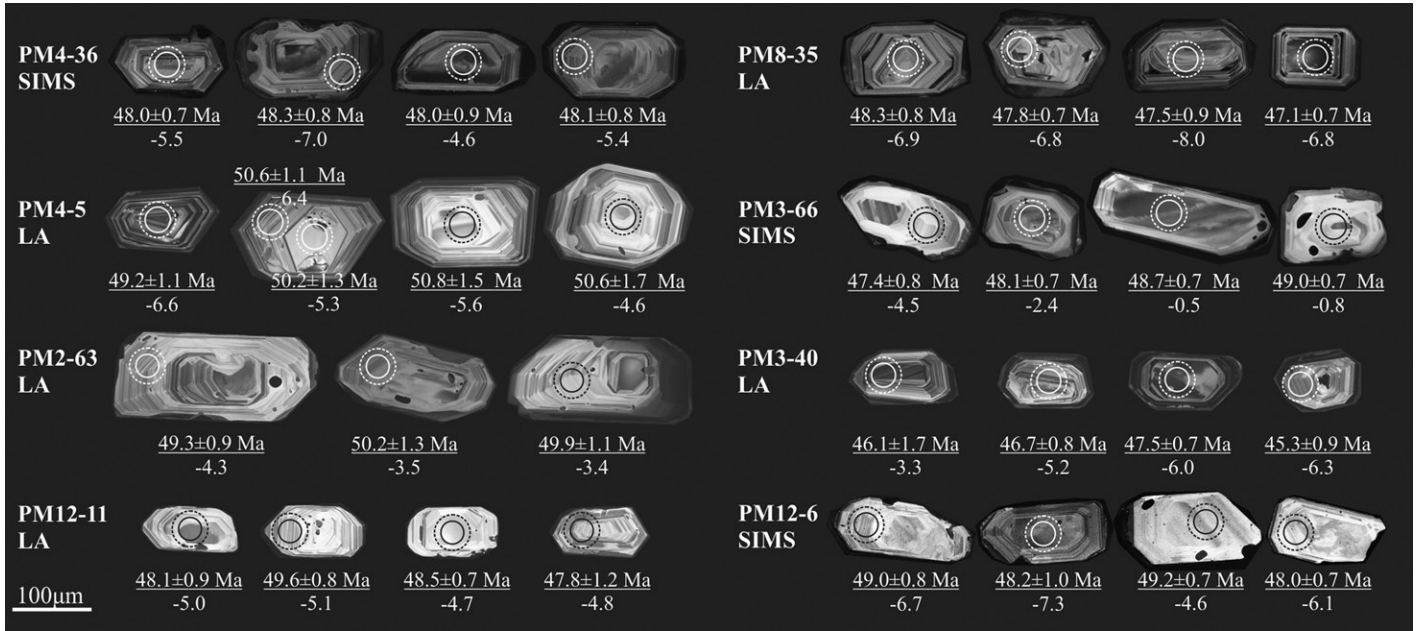


Figure 3. Cathodoluminescence images for representative zircon grains from the Lopu Range batholith, Tibet. Solid and dashed circles indicate the spot locations of U-Pb age and in situ Hf isotope analyses, respectively. SIMS—secondary ion mass spectrometry; LA—laser ablation.

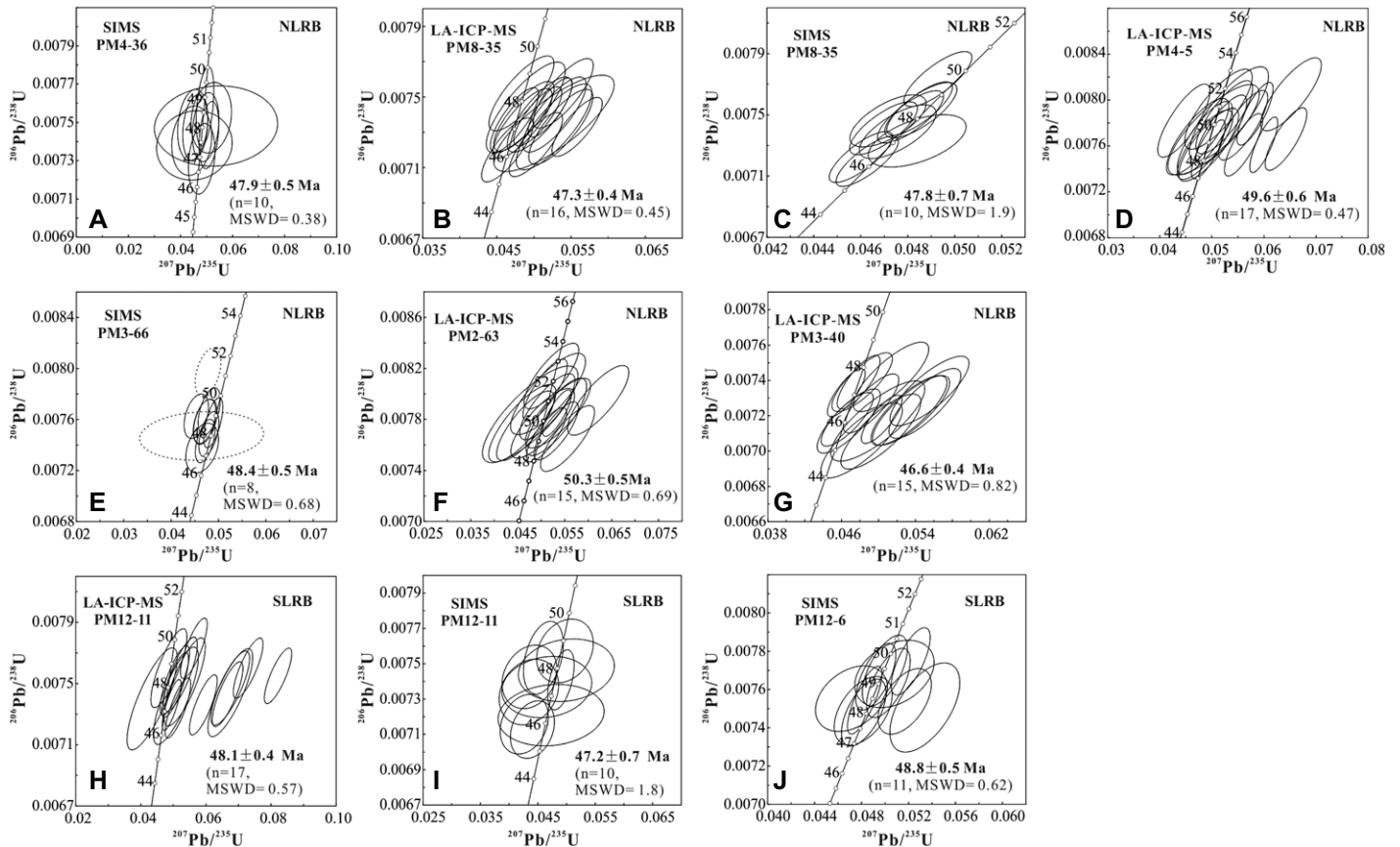
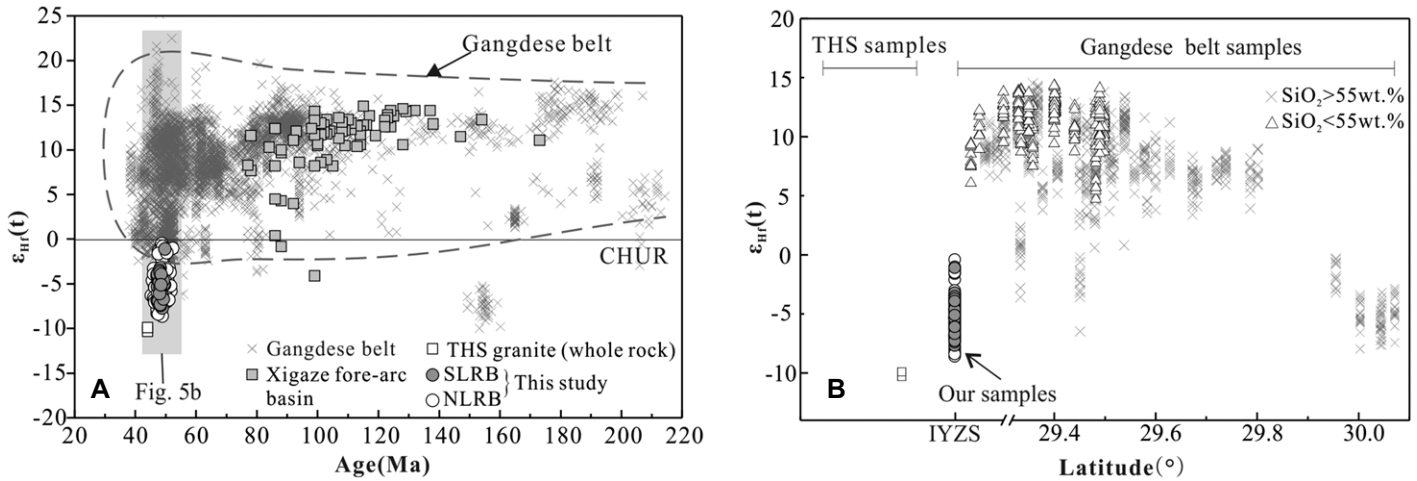


Figure 4. Zircon U-Pb concordia diagram for the Lopu Range batholith, Tibet (Table S1; see footnote 1). SIMS—secondary ion mass spectrometry; LA-ICP-MS—laser ablation—inductively coupled plasma—mass spectrometry; n—Number of zircon grains; MSWD—mean square weighted deviation; NLRB—the Lopu Range batholith north of the IYZS; SLRB—the Lopu Range batholith south of the IYZS.



**Figure 5.** (A) Plot of  $\epsilon_{\text{Hf}}(t)$  versus U-Pb ages for zircon. The results on 200–40 Ma zircons from granitoids to basaltic rocks in the eastern Gangdese belt, Tibet and whole rock Hf isotope of early Eocene granite in the Himalaya are presented for comparison. Data sources are listed in Data 1 and supplementary file (see footnote 1). (B)  $\epsilon_{\text{Hf}}(t)$  plotted against the latitude of the samples analyzed in the eastern Gangdese belt. The detailed GPS data for the sampling localities are listed in Data 2 (see footnote 1). CHUR—chondritic uniform reservoir; THS—Tethyan Himalaya Sedimentary Sequences; IYZS—Indus-Yarlung Zangbu suture; NLRB—the Lopu Range batholith north of the IYZS; SLRB—the Lopu Range batholith south of the IYZS.

have more enriched Sr and Nd isotopic ratios ( $^{87}\text{Sr}/^{86}\text{Sr}_i = 0.70944\text{--}0.71213$  and  $\epsilon_{\text{Nd}}(t) = -7.3$  to  $-9.8$ ) than other Jurassic to Eocene Gangdese rocks (Fig. 8A). The samples from the SLRB have  $^{87}\text{Sr}/^{86}\text{Sr}_i = 0.71200\text{--}0.71226$ , and  $\epsilon_{\text{Nd}}(t)$  values ( $-8.2$  to  $-8.0$ ), which are similar to those of the NLRB (Fig. 8A). Given that all of the samples analyzed have relatively high  $^{87}\text{Rb}/^{86}\text{Sr}$  values (typically  $>2$ ), the calculated errors on the initial  $^{87}\text{Sr}/^{86}\text{Sr}$  values are shown in Figure 8B.

**DISCUSSION**

**Source Characteristics of the Lopu Range Batholith (LRB)**

The published zircon U-Pb ages (Laskowski et al., 2017), together with our new results, indicate that the LRB is dominated by 50–47 Ma granitoids, with minor 38 Ma granite, and 16 Ma two-mica leucogranite dikes (Fig. 1B). Our study focused on the 50–47 Ma rocks in the LRB. The field investigation and zircon U-Pb

data indicate that the NLRB was emplaced into the southern Lhasa terrane at 50–47 Ma, and the SLRB intruded into the siliciclastic matrix mélangé strata at 49–47 Ma. These results are analytically indistinguishable and they are taken to confirm that the different analyzed portions of the batholith represent a single magmatic event.

High  $\text{SiO}_2$  ( $>64$  wt%) and low  $\text{Mg}^\#$  (17–52) are generally considered to reflect partial melting of crustal materials or assimilation and fractional crystallization (AFC) of basaltic magmas. We suggest that the LRB were not generated by AFC

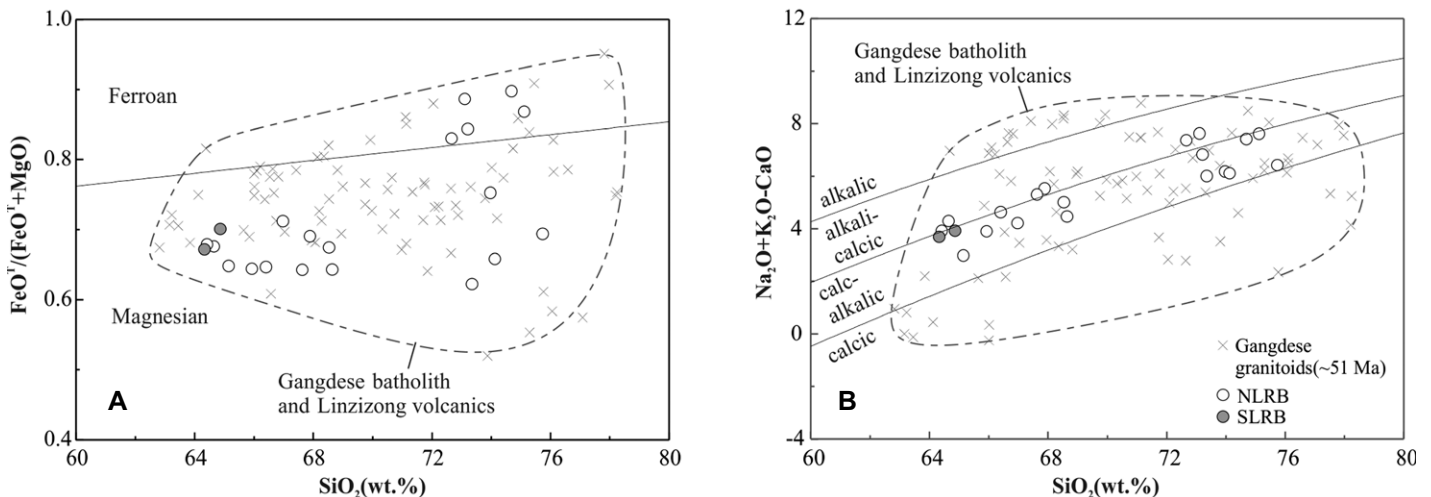


**Figure 6.** (A)  $\text{FeO}^T/(\text{FeO}^T + \text{MgO})$  vs  $\text{SiO}_2$  diagram, and (B)  $(\text{Na}_2\text{O} + \text{K}_2\text{O} - \text{CaO})$  against  $\text{SiO}_2$  diagram (after Frost et al., 2001). For comparison, the fields for the ca. 51 Ma Gangdese rocks and Linzizong volcanic rocks (Tibet) are from Mo et al. (2008), Lee et al. (2012), Bouilhol et al. (2013), Wang et al. (2015), Zhu et al. (2015), and Liu et al. (2018). NLRB—the Lopu Range batholith north of the Indus-Yarlung Zangbu suture; SLRB—the Lopu Range batholith south of the Indus-Yarlung Zangbu suture.

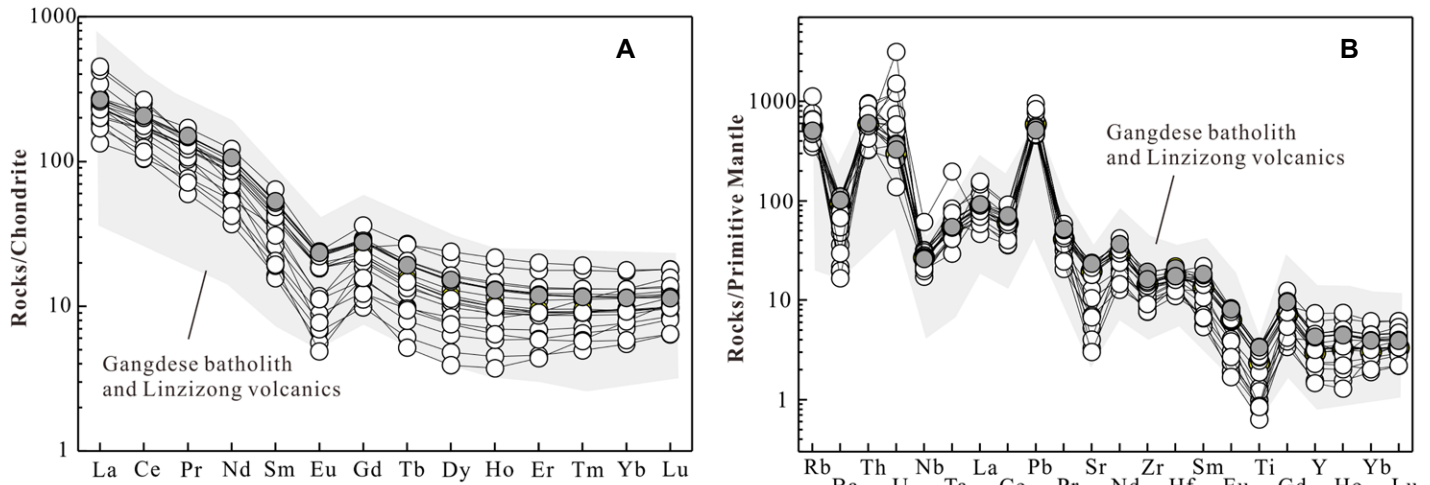


**Figure 7. (A) Chondrite-normalized rare earth element and (B) primitive-mantle normalized trace element patterns for Lopu Range batholith, Tibet (Normalizing values are from Sun and McDonough, 1989), data sources of ca. 51 Ma Gangdese rocks and Linzizong volcanic rocks are the same as Figure 6.**

of basaltic magmas for a number of reasons. Fractional crystallization experiments of basaltic melts indicate that evolved melts become peraluminous ( $A/CNK > 1$ ) at  $SiO_2$  contents of 54–65 wt% (Grove et al., 2003; Pichavant and Macdonald, 2007; Ulmer et al., 2018). Our samples are metaluminous ( $A/CNK < 1$ ) with  $SiO_2$  ranging from 64 to 73 wt% (Table S2), suggesting that they were not derived by fractional crystallization of basaltic magmas. There is also no correlation between  $SiO_2$  contents (64–76 wt%) and  $\epsilon_{Nd}(t)$  values (–7.3 to –9.8) (not shown), further indicating that the LRB were not produced by AFC of basaltic magmas.

If the LRB were derived by partial melting of the crustal materials, its high  $K_2O$  contents (4.1–5.3 wt%) and  $K_2O/Na_2O$  ratios (1.31–1.92) indicate its source rocks had relatively high K contents (Sisson et al., 2005), since low-K source rocks tend to produce low  $K_2O$  melts ( $K_2O < 4$  wt%, Rapp and Watson, 1995; Gao

et al., 2016). The inverse correlation between  $SiO_2$  and  $P_2O_5$  indicates that the LRB is an I-type granitoid (Figs. S2A and S2E) (Chappell and White, 1992). All samples have low  $(Gd/Yb)_N$  (0.9–2.7) ratios and relatively flat heavy rare earth element (REE) patterns (Fig. 7A; Table S2), indicating that garnet, which would result in strong depletion of heavy REE relative to middle REE, was not a major residual mineral and that melting pressure was probably  $< 1.5$  GPa (Pertermann et al., 2004). Systematic variation of different elements versus  $SiO_2$  (Fig. S2) suggests that the high  $SiO_2$  granite was produced by fractional crystallization of low  $SiO_2$  quartz monzonite. For example, the negative correlation between  $SiO_2$  and  $Eu/Eu^*$  (Fig. S2G), and the positive correlation between  $SiO_2$  and Rb/Sr ratios (Fig. S2H) are consistent with fractional crystallization of plagioclase. Zircon fractionation might in turn be responsible for the low Zr/Hf ratios in the granites (Fig. S2I) (Linnen and

Keppler, 2002). Therefore, we propose that the LRB resulted from partial melting of a relatively K-rich crustal source, consistent with its elevated initial Sr isotope ratios ( $^{87}Sr/^{86}Sr_i = 0.70944–0.71213$ ), followed by fractional crystallization. The source Rb/Sr values = 0.17–0.25, calculated by the method of Dhuime et al. (2015).

#### Ages of Early India Continental Subduction in the Central Himalaya

The high-pressure to ultrahigh-pressure (HP–UHP) complexes in the Himalaya provide robust geologic evidence for subduction of Indian continental material. The UHP complexes, with peak pressures of 4.4–4.8 GPa at  $\sim 560–760$  °C, are only known from the Kaghan area in Pakistan and the Tso Moriri areas of India adjacent to the western Himalaya syntaxis (e.g., Guillot et al., 2008; Wilke et al., 2015). The Kaghan Valley UHP event is dated by U–Pb dating of zircon rims containing coesite inclusions at 46.2 Ma (Kaneko et al., 2003), consistent with initial Indian continent subduction by 51 Ma or soon thereafter (Donaldson et al., 2013). For the Tso Moriri rocks, although the timing of UHP metamorphism is still uncertain, in that there are age peaks at 53–51 Ma (de Sigoyer et al., 2000; Leech et al., 2005; St-Onge et al., 2013) and at 47–46 Ma (Donaldson et al., 2013), it appears that the Indian continent began to subduct prior to 50 Ma. These results therefore indicate that subduction of Indian continental crust had commenced before 51 Ma across the western Himalaya. In contrast UHP complexes are absent in the central and eastern Himalaya, and the HP metamorphic rocks show unexpectedly young ages of peak metamorphism ( $\leq 40$  Ma)

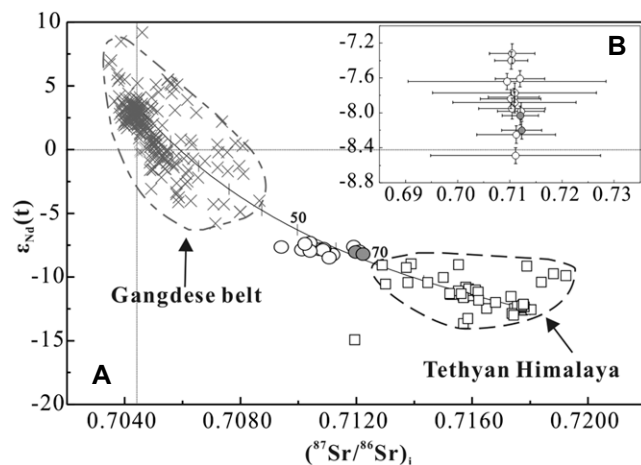


**Figure 8. Whole rock Sr–Nd isotope ratio diagram for Lopu Range batholith, Gangdese belt and Tethyan Himalaya Sedimentary (the data are listed in Data 3; see footnote 1). The Sr–Nd isotope ratios with calculated errors are shown in Figure 8B.**



compared with those from the western Himalaya (e.g., Zhang et al., 2015; Laskowski et al., 2016). In the central Himalaya, HP rocks were largely retrogressed after ca. 42 Ma, but relict assemblages (Phe + Chl ± Sta ± Grt-bearing) indicate a peak pressure of >1.4 GPa at <600 °C in the Lopu Range area (Laskowski et al., 2016). In the eastern Himalaya, the HP granulites from the eastern Himalaya Syntaxis experienced peak-metamorphism of 1.3–1.6 GPa and 840–880 °C at 40–30 Ma (zircon U-Pb ages, Zhang et al., 2015). Although these results suggest that Indian crust was also subducted after the initial India-Asia collision (at 59 Ma in the central-eastern Himalaya, DeCelles et al., 2014; Hu et al., 2015, 2016 and references therein), we do not yet have other geological evidence for any older (>40 Ma) continental subduction in the central-eastern Himalaya.

We conclude that the LRB records the subduction of Indian continental crust in the central Himalaya before ca. 50 Ma based on the following evidence: field investigations confirm that the LRB intruded into the IYZS, indicating that our samples were emplaced at the India-Asia collisional boundary. Given that the ages of the LRB are younger than the age of initial collision of India and Asia in the central Himalaya (59 Ma, DeCelles et al., 2014; Hu et al., 2015, 2016 and references therein), the southern Lhasa terrane and subducted Indian crust are both potential source materials for the LRB. In the Lopu Range area, detrital zircon U-Pb ages from the Xigaze fore-arc basin were dominated by Mesozoic and 53 of the 77 zircons analyzed have positive zircon  $\epsilon_{\text{Hf}}(t)$  values (Fig. 5A). The Sangdanlin section in the Tethyan Himalaya, which is close to the Lopu area, has a typical stratigraphic section used to constrain the timing of the India-Asia collision. It contains Paleocene positive zircon  $\epsilon_{\text{Hf}}(t)$  values, similar to the Gangdese batholith (DeCelles et al., 2014; Wu et al., 2014). In addition, a 57 Ma granite, located 20 km west of the Lopu Range area, has  $^{87}\text{Sr}/^{86}\text{Sr}_i = 0.7056$ ,  $\epsilon_{\text{Nd}}(t) = -0.1$  and zircon  $\epsilon_{\text{Hf}}$  isotope values of 0.1–3.9 (Zhang, 2018), overlapping the Sr-Nd-Hf isotope compositions of the Gangdese batholith and the Linzizong volcanic succession (Figs. 5A and 8). Thus the Lopu Range area was characterized by juvenile crust prior to the India-Asia collision, consistent with the results of previous studies, highlighting that the southern Lhasa terrane is mostly juvenile crust with depleted Sr-Nd-Hf isotopic values (Chu et al., 2011; Zhu et al., 2011, 2013; Hou et al., 2015; Zhou et al., 2017).

The THS crustal basement, in contrast, has enriched isotopic compositions that differ from those of the southern Lhasa terrane (Figs. 5 and 8). If the LRB was derived from the southern Lhasa terrane or the THS, then the granitoids

should display corresponding isotopic compositions. However, all our samples have similar Sr-Nd-Hf isotope compositions that are intermediate between those of the southern Lhasa terrane and the THS (Figs. 5 and 8). Therefore, neither the southern Lhasa terrane nor the THS crust appears to have been the sole source of the LRB. Rather, we argue that the LRB was generated by partial melting of a mixed source containing both Indian continental material and southern Lhasa terrane juvenile crust. A simple two end-member mixing calculation between the average composition of Gangdese belt and THS middle-lower crust (represented by Eocene granite in the Himalaya) (Fig. 8A) indicates that the LRB could have been derived from a mixture of 50%–70% enriched Indian crust and 30%–50% juvenile southern Lhasa middle-lower crust. This highlights that Indian continental crust had already been subducted beneath the mid to lower crust of southern Lhasa terrane when the partial melting occurred, supporting the view that Indian continental subduction took place before 51 Ma.

### Geodynamic Processes Responsible for the Lopu Range Batholith (LRB)

Some continental arcs appear to be characterized by high volume magmatic episodes separated by magmatic lulls (DeCelles et al., 2009, 2015 and references therein). The Gangdese arc rocks resulted from the northward subduction of the Neo-Tethyan oceanic slab and subsequent India-Asia collision and Indian continental subduction along the southern margin of the Lhasa terrane (Chang and Zheng 1973; Allègre et al., 1984; Debon et al., 1987; Chung et al., 2005; Chu et al., 2011; Zhu et al., 2011, 2015, 2019). The 52–48 Ma rocks (here termed the ca. 51 Ma high volume event) appear to have been the largest and most widespread magmatic episode within the Gangdese arc. They are pre-dominantly I-type intrusive granites with minor mafic rocks, together with the Linzizong subduction-related volcanic successions, and the magmas were largely derived from within the continental lithosphere (Guo et al., 2007; Wang et al., 2015; Zhu et al., 2015, 2019). The age of the initial India-Asia collision, constrained by the Asia-derived sediments deposited on the Indian plate, is 59 Ma in the central-eastern Himalaya and 54 Ma in the western Himalaya (DeCelles et al., 2014; Hu et al., 2015; Najman et al., 2017). The ca. 51 Ma high volume event, therefore, reflects a pulse of increased magmatic activity after continental collision and presumably while both Indian continental material and Neo-Tethyan oceanic crust were being subducted. It also appears that the ca. 51 Ma high volume event occurred during the period of Indian continental subduction and that

it was shorter than magmatic pulses associated with oceanic subduction (10–30 Ma, DeCelles et al., 2009, 2015). The majority of magmas were derived from within the lithosphere, and published data sets further demonstrate that ca. 51 Ma intermediate-acid rocks in the Gangdese belt tend to have higher and greater variations in whole rock zircon saturation temperatures ( $T_{\text{Zr}} = 680\text{--}900$  °C) than those generated between 55 and 70 Ma (600–770 °C, Wang et al., 2015; Zhu et al., 2015; Liu et al., 2018). In the eastern Himalaya, a 45 Ma (Titanite U-Pb age) oceanic island basalt (OIB)-type gabbro has been reported with a high magmatic temperature (1380 °C, Ji et al., 2016). The high volume of magmatic rocks (including minor mafic rocks) with relatively high magma temperatures, is therefore thought to have been linked to increased mantle heat into the lithosphere (Zhu et al., 2015). The ages of the LRB place it within the ca. 51 Ma high volume event of the Gangdese belt, indicating that generation of the LRB was associated with this large-scale magmatic event.

Along destructive plate margins, upwelling of asthenosphere can be triggered by oceanic slab break-off (Davies and von Blanckenburg, 1995; Zhu et al., 2015; Ji et al., 2016) and by foundering of segments of thickened lithosphere mantle from the overlying plate (Kapp et al., 2007; DeCelles et al., 2009, 2015), and the thermal consequences are likely to be different. Thermal anomalies resulting from slab break-off tend to be related to the depth of break-off (Davies and von Blanckenburg, 1995; van de Zedde and Wortel, 2001; Baumann et al., 2010; Freeburn et al., 2017). Whereas break-off at depths shallower than the base of overlying lithosphere plate is more likely to generate magmas in the overlying plate (Davies and von Blanckenburg, 1995; van de Zedde and Wortel 2001), deeper slab break-off may not lead to a significant thermal perturbation and hence not result in significant magmatism (Davies and von Blanckenburg, 1995; Baumann et al., 2010; Freeburn et al., 2017). Between 68 and 51 Ma, the India-Asia convergence rate was around 15 cm/yr (Patriat and Achache, 1984; van Hinsbergen et al., 2011). If the initial India-Asia collision occurred at 59 Ma (e.g., DeCelles et al., 2014; Hu et al., 2015), then a constant India-Asia convergence rate between 59 and 51 Ma would suggest that the subducted Indian lithosphere provided a negative buoyancy similar to a downgoing oceanic slab, in order to maintain the velocity of the Indian plate (Capitanio et al., 2010). For such convergence rates, the leading edge of the Indian continent would have reached depths of 300 km, 425 km, and 520 km with subduction dips of 30°, 45°, and 60°, respectively, 4 Ma after the India-Asia collision. If oceanic slab break-off then occurred

at such depths, it is likely that there was little thermal perturbation and hence no magmatism (Freeburn et al., 2017). Overall, there is therefore little reason to invoke slab break-off as a cause of the ca. 51 Ma high magma volume episode.

Instead we employed a numerical model from Huangfu et al. (2018), that focuses on the thermal evolution from oceanic to continental subduction, to investigate the source of additional heat for the high-volume magmatic event during continental subduction (Fig. 9; Fig. S3 [see footnote 1], from Mode-II in Huangfu et al., 2018). The setup parameters and methods are as in Huangfu et al. (2018) and their supplementary files. In this model, once continental subduction was initiated (from 11 to 40 m.y. after commencement of the model, Figs. 9A and 9B; Fig. S3), the temperature in the overlying plate crust remained constant and it was

still lower than the  $T_{Zr}$  of the LRB (678–746 °C) and other Gangdese rocks (680–900 °C). This suggests that subduction of the Indian lithosphere resulted in little heating within the orogen, and it is an unlikely cause of extensive partial melting of lithosphere in the overlying plate. However, if a portion of the overlying plate lithosphere were to founder at, say 53 m.y. after the model started (Figs. 9C and 9D), then the temperature of the crust would increase significantly in a relatively short time (1–2 m.y.). Thus, if lithosphere delamination occurred beneath the Gangdese arc belt, this would have resulted in extra heating from the upwelling asthenosphere. Recent seismic studies have observed the high-V structure beneath the Lhasa terrane, which was attributed to foundering continental lithosphere (e.g., Chen et al., 2017). We conclude that the removal of

the Lhasa lithosphere mantle was initiated in the Eocene, and that this resulted in upwelling of asthenosphere, which is the main source of additional heat for the ca. 51 Ma high volume magmatism in southern Tibet. The Lhasa terrane experienced more than 50% crustal shortening between 90 and 69 Ma, resulting in a thickened and gravitationally unstable lithosphere before the India-Asia collision (Kapp et al., 2007). After the India-Asia collision, subduction of the India continent continued to compress the thickened lithosphere, facilitating detachment from the base of the lithosphere, and eventually contributing to lithosphere delamination. This resulted in the ca. 51 Ma magmatism, including the OIB-type mafic rocks (Ji et al., 2016), and it contributed to uplift of the Gangdese belt during the Eocene (Kapp et al., 2007; Li et al., 2015).

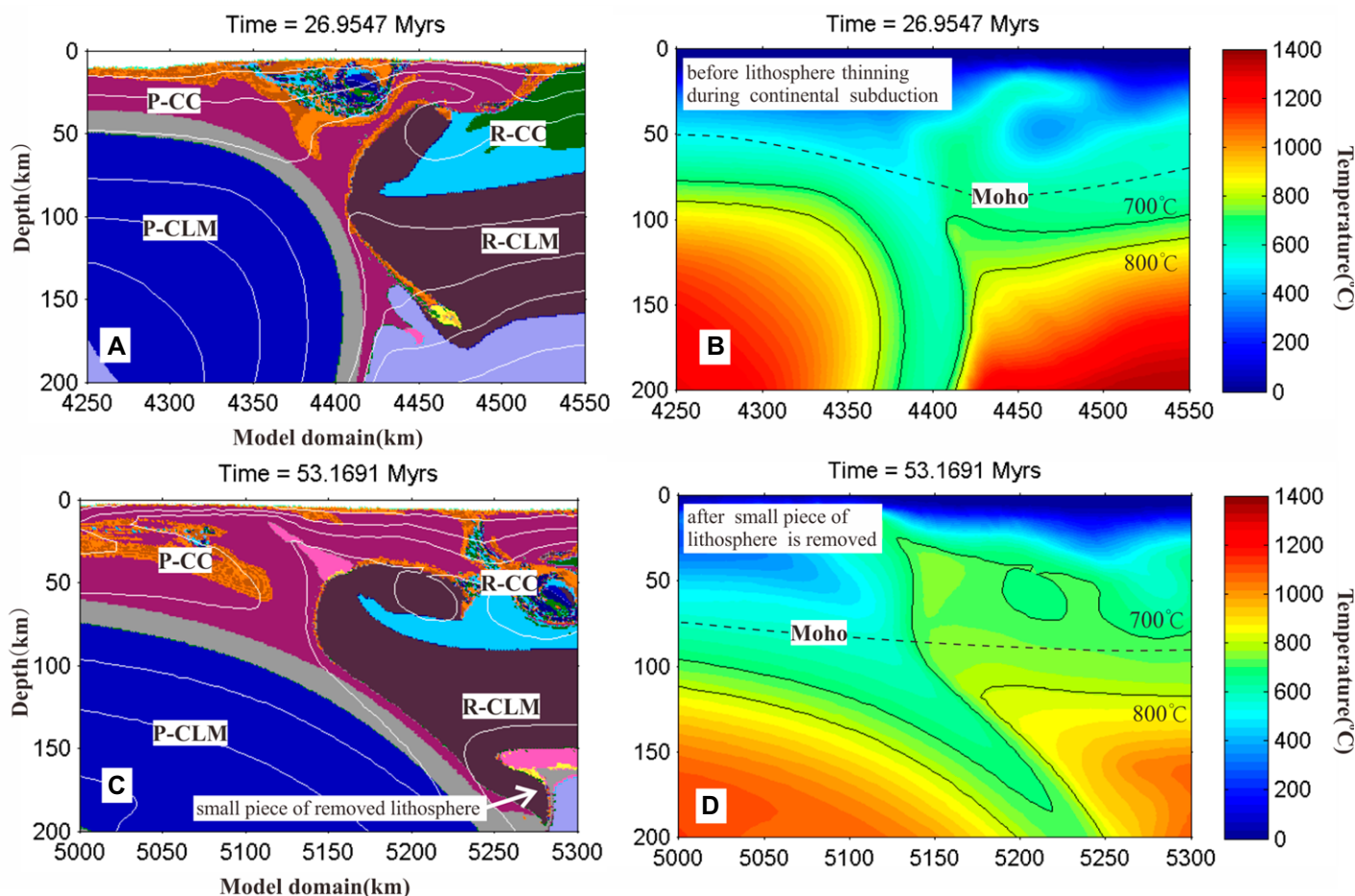


**Figure 9.** A thermal model for the transition from oceanic to continental subduction from Huangfu et al. (2018). The model result is shown in Figure S3 (see footnote 1). The Time captions in the figure represent the run times in the model. When  $T < 11$  Ma, oceanic subduction was occurring, and at  $T \geq 11$  Ma, continent collision occurred and continental subduction started. (A–D) Illustrate the thermal state before and after the lithosphere thinning during continental subduction, and the black lines are the 700 and 800 °C isotherms. The illustrations on the left are images of the continental subduction and those on the right show the corresponding isothermal state. The setup parameters and methods are listed in Huangfu et al. (2018). P-CC—Pro-continental crust; P-CLM—Pro-continental lithospheric mantle; R-CC—Retro-continental crust; R-CLM—Retro-continental lithospheric mantle.

**Implications for the Initial Geometry of Indian Continental Subduction**

According to the HP-UHP metamorphic records, initial Indian continental subduction was shallow (flat) in the eastern Himalaya but steep in the western Himalaya (Guillot et al., 2008). Here, the composition and the distribution of the ca. 51 Ma magmatism in the eastern Gangdese belt (85°E to 94°E) and the results of our study on the LRB are used to constrain the geometry of Indian continental subduction in the central-eastern Himalaya.

Subduction of Indian crustal materials with enriched isotopic compositions (Figs. 5 and 8) to subarc depths after 59 Ma along a shallow subduction zone, would have released fluids and/or melts enriched in incompatible elements from the subducted crust into the Asia lithosphere (Mahéo et al., 2009; Hermann et al., 2013, Zheng and Chen, 2016). This resulted in an enriched mantle source, that was different from that metasomatized by the Neo-Tethyan oceanic slab which had depleted Sr-Nd-Hf isotope ratios, beneath the Lhasa terrane (Mahéo et al., 2009). Previous studies suggest that the zircon  $\epsilon_{\text{Hf}}$  values of granitoids ranged toward negative values in the ca. 51 Ma magmatic rocks of southern Lhasa, and that this reflects either (1) the mixing of Himalaya sediments with the mantle wedge following the convergence between India and Asia (Chu et al., 2011; Zhu et al., 2015) or (2) the reworking of ancient Lhasa basement (e.g., Zhang et al., 2019). The former model stresses that the basalts from mixed sources remelted and in turn differentiated to form the Gangdese granitoids with negative zircon  $\epsilon_{\text{Hf}}$  values. However, the ca. 51 Ma basaltic rocks in the eastern Gangdese belt have positive zircon  $\epsilon_{\text{Hf}}$  values, while the intermediate-felsic rocks have widely variable  $\epsilon_{\text{Hf}}$  values and there is no correlation between  $\epsilon_{\text{Hf}}$  values and their latitude (Fig. 5B). This suggests that the mantle source of ca. 51 Ma basaltic rocks did not contain contributions from the subducted Indian materials. We note that the ca. 51 Ma rocks occur north of the IYZS in the eastern Gangdese belt, and the granites with negative zircon  $\epsilon_{\text{Hf}}$  values outcrop in the adjacent Linzhi area (Chu et al., 2011) and Dajiacuo area (Zhang et al., 2019), where ancient Lhasa basement was present (Zhu et al., 2013; Zhang et al., 2019).

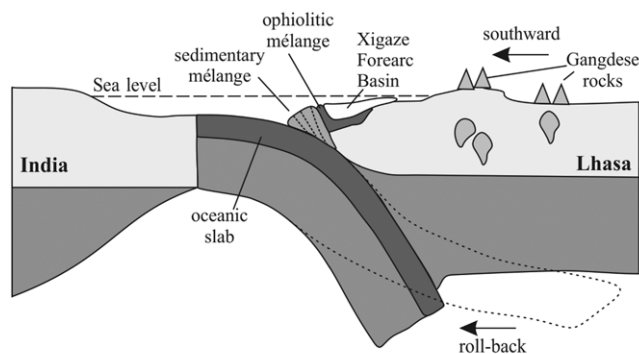
In the Lupu Range and adjacent areas, only the LRB intruded into the IYZS has enriched zircon Hf isotope ratios, while other ca. 51 Ma rocks, distributed north of the IYZS, have zircon  $\epsilon_{\text{Hf}}$ (t) values of -2 to +5 (Zhu et al., 2011; Hou et al., 2015). In the western Gangdese belt, ca. 51 Ma granitoids also occurred north of the IYZS, and they have positive zircon  $\epsilon_{\text{Hf}}$ (t) and whole rock  $\epsilon_{\text{Nd}}$ (t) values (Bouilhol et al., 2013; Wang et al.,

2015). These results indicate that over most of the area the magmatic rocks of the Gangdese belt maintained a juvenile crustal signature after the India-Asia collision. Thus, the negative zircon  $\epsilon_{\text{Hf}}$  values in the volumetrically minor ca. 51 Ma felsic rocks north of the IYZS are thought to have been inherited from the ancient Lhasa crust (Xu et al., 2013; Zhang et al., 2019), rather than from a mixture that included Indian continental materials. The removal of Asian lithosphere would have triggered the melting of juvenile and ancient Lhasa crust, contributing to the large variation of zircon  $\epsilon_{\text{Hf}}$  values in the felsic rocks (Fig. 5B).

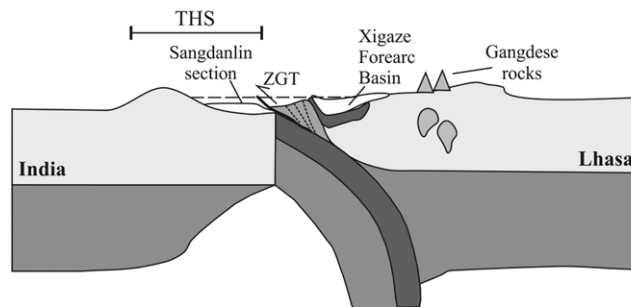
Considering the geometry of the oceanic slab and compositional variation of Gangdese rocks,

we propose a steep (or vertical) subduction of Indian continent lithosphere around 50 Ma in the central-eastern Himalaya. Zhu et al. (2019) reconstructed the geometry of the Neo-Tethyan oceanic subduction since 120 Ma. In the Gangdese belt, the southward propagation of Gangdese magmatism after 70 Ma suggests that there was subduction roll-back with associated steepening of the Neo-Tethyan oceanic slab (Fig. 10A). The Xigaze forearc basin, which was deposited on an ophiolite basement, received terrigenous detritus from the Gangdese belt and transitioned from underfilled to filled between 89 and 59 Ma (Wu et al., 2010; Orme et al., 2015; Orme and Laskowski, 2016). The sedimentary mélangé

**A ~ 65 Ma subduction roll-back of Neo-Tethyan oceanic slab**



**B 59 Ma India-Asia collision**



**C ~53 Ma lithosphere delamination produced the ~51 Ma magma**

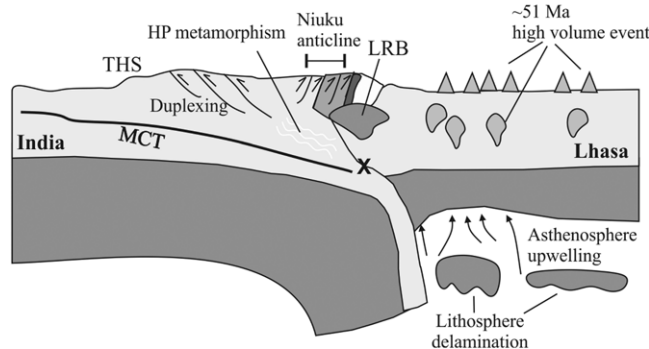


**Figure 10. Schematic cross sections illustrating the transition from Tethyan oceanic slab subduction to early India continental subduction. (A) Roll-back of the Tethyan oceanic slab after 65 Ma (Chung et al., 2005; Wang et al., 2015; Zhu et al., 2015, 2019). (B) After the initial India-Asia collision, the sedimentary mélangé was thrust southward (Zongba-Gyangze Thrust system, ZGT) onto the northern Indian continental margin, and the Tethyan Himalaya Sedimentary Sequences (THS) started to receive Asian derived detritus, forming the Sangdanlin strata. Subduction of Indian continental lithosphere started at this stage. (C) The ongoing convergence between Asia and India resulted in the contraction of THS and Lhasa strata and the formation of the Niuku anticline. Lithosphere delamination at ca. 53 Ma induced partial melting in the mantle lithosphere and the crust, producing the ca. 51 Ma high volume magmatic event including the Lupu Range batholith. “X” represents the inferred crustal source of the Lupu Range batholith.**

formed along the southern margin of Asia by accretion of rocks from the oceanic plate mixed with terrigenous detritus from the Xigaze forearc basin (Searle et al., 1987; Zhu et al., 2005; Cai et al., 2012; An et al., 2017; Metcalf and Kapp, 2017, 2019; Wang et al., 2017a, 2018).

After the India-Asia collision at ca. 59 Ma in the central-eastern Himalaya (Hu et al., 2016 and references therein), the Zhongba-Gyangze Thrust emplaced the sedimentary mélange in the hanging wall southward onto the THS of the northern Indian continental margin in the footwall (Fig. 10B, Ding et al., 2005; Wang et al., 2017a). The THS started to receive Asian derived detritus as recorded in the Sangdanlin sediments (Ding et al., 2005; DeCelles et al., 2014; Wu et al., 2014; Hu et al., 2015). The subducted Indian crust was readily subducted after its mid-upper crust was scrapped off (duplexing) (Fig. 10C, Capitanio et al., 2010), and exhumation of subducted Indian mid-crust recorded HP metamorphism that was ongoing by 40 Ma (Zhang et al., 2015; Laskowski et al., 2016). The continuing convergence between Asia and India resulted in compaction of the THS and IYZS strata, with south-directed thrusting and the formation of the Niuku anticline before 45 Ma in the Lopu Range area (Figs. 1D and 10C, Ding et al., 2005). The rate of India-Asia convergence did not change significantly between 59–51 Ma (Patriat and Achache, 1984; van Hinsbergen et al., 2011), suggesting that the subducted Indian continent would have advanced the steepening process with roll-back rather than underplating. During this stage, the Indian continent was not subducted beneath the Lhasa lithosphere, and so the depleted mantle modified by Neo-Tethyan oceanic subduction beneath the southern Lhasa would have retained its geochemical features during Indian continental subduction (Fig. 10C).

Around ca. 53 Ma (presumed age), lithosphere delamination occurred beneath the Lhasa terrane, triggering partial melting of the overlying lithosphere from the Himalaya to the Lhasa terrane at ca. 51 Ma (Fig. 10C). Melting in the different tectonic units would have generated distinct geochemical compositions. Melting of juvenile and ancient Lhasa crust produced intermediate-felsic rocks with both depleted and evolved Sr-Nd-Hf isotopic compositions, whereas the mantle-derived mafic rocks maintain their depleted Sr-Nd-Hf isotopic values (Figs. 5B and 8). In the Lopu Range region, partial melting of mixed crust produced the LRB that intruded into the sedimentary mélange, displaying intermediate isotope ratios between those of the southern Lhasa terrane and the India continent (Figs. 5 and 8 and “X” in Fig. 10C). While Indian continental material was subducted at a steep angle, little subducted Indian

crust would have been added to the Asia lithosphere (Fig. 10C). Therefore, we conclude that early, steep angle continental subduction took place between the onset of India-Asia collision (59 Ma) and 46 Ma along the central-eastern India-Asia boundary.

## CONCLUSIONS

We report new geochemical data on a syn-tectonic, post-collisional batholith that crosscuts rocks on both sides of the central Indus-Yarlung Zangbu suture zone. On the basis of the new data and the geochemical composition and distribution of high volume ca. 51 Ma magmatism in the Gangdese belt, our conclusions are summarized as follows:

(1) The Lopu Range batholith was emplaced into the Indus-Yarlung Zangbu suture between  $50.3 \pm 0.5$  and  $46.6 \pm 0.4$  Ma.

(2) The magma source of the Lopu Range batholith was a mixture of juvenile Gangdese and isotopically enriched Indian crustal materials highlighting that Indian crustal material had been subducted by 50 Ma.

(3) The removal of Asian lithospheric mantle triggered the ca. 51 Ma high volume event along the Gangdese belt.

(4) Steeply dipping Indian continental subduction occurred along the central and eastern Himalaya between 59 and 46 Ma.

## ACKNOWLEDGMENTS

The Editor-in-Chief Professor Wen-Jiao Xiao, Associate Editor, Dr. Kate Metcalf and an anonymous reviewer are acknowledged for their reviews on the manuscript. The Gweltaz Mahéo, Mary Leech, and Andrew K. Laskowski are acknowledged for their insightful and constructive reviews of a previous version of the manuscript. We thank Pengpeng Huangfu, Zhonghai Li, and Taras Gerya for the numerical modeling and provision of the model results with the code of “I2VIS.” Financial support for this research was provided by the Second Tibetan Plateau Scientific Expedition and Research (2019QZKK0702), the National Natural Science Foundation of China (nos. 91855215 and 41630208), the Key Program of the Chinese Academy of Sciences (QYZDJ-SSW-DQC026), the Strategic Priority Research Program (A) of the Chinese Academy of Sciences (no. XDA2007030402), the National Key Research and Development Program of China (no. 2016YFC0600407), and Guangzhou Institute of Geochemistry Chinese Academy of Sciences (GIGCAS) 135 project 135TP201601. CJH acknowledges support from Leverhulme Trust grants RPG-2015-422 and EM-2017-0474. Y. Qi acknowledges support from China Scholarship Council (no. 201704910602). This is contribution no. IS-2890 from GIGCAS.

## REFERENCES CITED

Ahmad, T., Harris, N., Bickle, M., Chapman, H., Bunbury, J., and Prince, C., 2000, Isotopic constraints on the structural relationships between the Lesser Himalayan Series and the High Himalayan Crystal-

line Series, Garhwal Himalaya: Geological Society of America Bulletin, v. 112, p. 467–477, [https://doi.org/10.1130/0016-7606\(2000\)112<467:ICOTSR>2.0.CO;2](https://doi.org/10.1130/0016-7606(2000)112<467:ICOTSR>2.0.CO;2).

- Allègre, C.J., Courtillot, V., Tapponnier, P., Hirn, A., Mattauer, M., Coulon, C., Jaeger, J.J., Achache, J., Schärer, U., Marcoux, J., Burg, J.P., Girardeau, J., Armijo, R., Gariépy, C., Gopel, C., Li, T.D., Xiao, X.C., Chang, C.F., Li, G.Q., Lin, B.Y., Teng, J.W., Wang, N.W., Chen, G.M., Han, T.L., Wang, X.B., Den, W.M., Sheng, H.B., Cao, Y.G., Zhou, J., Qiu, H.R., Bao, P.S., Wang, S.C., Wang, B.X., Zhou, Y.X., and Ronghua, X., 1984, Structure and evolution of the Himalaya-Tibet orogenic belt: *Nature*, v. 307, p. 17–22, <https://doi.org/10.1038/307017a0>.
- An, W., Hu, X., and Garzanti, E., 2017, Sandstone provenance and tectonic evolution of the Xiukang Mélange from Neotethyan subduction to India-Asia collision (Yarlung-Zangbo suture, south Tibet): *Gondwana Research*, v. 41, p. 222–234, <https://doi.org/10.1016/j.gr.2015.08.010>.
- Baumann, C., Gerya, T.V., and Connolly, J.A.D., 2010, Numerical modelling of spontaneous slab break-off dynamics during continental collision, *in* Spalla, M.L., Marotta, A.M., and Gosso, G., eds., *Advances in Interpretation of Geological Processes: Refinement of Multi-scale Data and Integration in Numerical Modelling*: Geological Society of London, Special Publications, v. 332, p. 99–114, <https://doi.org/10.1144/SP332.7>.
- Bouilhol, P., Jagoutz, O., Hanchar, J.M., and Dudas, F.O., 2013, Dating the India-Eurasia collision through arc magmatic records: *Earth and Planetary Science Letters*, v. 366, p. 163–175, <https://doi.org/10.1016/j.epsl.2013.01.023>.
- Cai, F., Ding, L., Leary, R.J., Wang, H.Q., Xu, Q., Zhang, L.Y., and Yue, Y.H., 2012, Tectonostratigraphy and provenance of an accretionary complex within the Yarlung-Zangpo suture zone, southern Tibet: Insights into subduction-accretion processes in the Neo-Tethys: *Tectonophysics*, v. 574–575, p. 181–192, <https://doi.org/10.1016/j.tecto.2012.08.016>.
- Capitanio, F.A., Morra, G., Goes, S., Weinberg, R.F., and Moresi, L., 2010, India-Asia convergence driven by the subduction of the Greater Indian continent: *Nature Geoscience*, v. 3, p. 136–139, <https://doi.org/10.1038/ngeo725>.
- Chang, C.F., and Zheng, X.L., 1973, Some tectonic features of the Mt. Jolmo Lungma area, southern Tibet, China: *Scientia Sinica*, v. 2, p. 257–265.
- Chappell, B.W., and White, A.J.R., 1992, I- and S-type granites in the Lachlan Fold Belt: *Transactions of the Royal Society of Edinburgh. Earth Sciences*, v. 83, p. 1–26, <https://doi.org/10.1017/S0263593300007720>.
- Chen, M., Niu, F., Tromp, J., Lenardic, A., Lee, C.-T.A., Cao, W., and Ribeiro, J., 2017, Lithospheric foundering and underthrusting imaged beneath Tibet: *Nature Communications*, v. 8, no. 15659, <https://doi.org/10.1038/ncomms15659>.
- Chen, Y., Li, W., Yuan, X., Badal, J., and Teng, J., 2015, Tearing of the Indian lithospheric slab beneath southern Tibet revealed by SKS-wave splitting measurements: *Earth and Planetary Science Letters*, v. 413, p. 13–24, <https://doi.org/10.1016/j.epsl.2014.12.041>.
- Chu, M.F., Chung, S.L., O'Reilly, S.Y., Pearson, N.J., Wu, F.Y., Li, X.H., Liu, D.Y., Ji, J.Q., Chu, C.H., and Lee, H.Y., 2011, India's hidden inputs to Tibetan orogeny revealed by Hf isotopes of Transhimalayan zircons and host rocks: *Earth and Planetary Science Letters*, v. 307, p. 479–486, <https://doi.org/10.1016/j.epsl.2011.05.020>.
- Chung, S.L., Chu, M.F., Zhang, Y.Q., Xie, Y.W., Lo, C.H., Lee, T.Y., Lan, C.Y., Li, X.H., Zhang, Q., and Wang, Y.Z., 2005, Tibetan tectonic evolution inferred from spatial and temporal variations in post-collisional magmatism: *Earth-Science Reviews*, v. 68, p. 173–196, <https://doi.org/10.1016/j.earscirev.2004.05.001>.
- Dai, J., Wang, C., and Li, Y., 2012, Relicts of the Early Cretaceous seamounts in the central-western Yarlung Zangbo Suture Zone, southern Tibet: *Journal of Asian Earth Sciences*, v. 53, p. 25–37, <https://doi.org/10.1016/j.jseas.2011.12.024>.

- Dai, J.G., Wang, C.S., Polat, A., Santosh, M., Li, Y.L., and Ge, Y.K., 2013, Rapid forearc spreading between 130 and 120 Ma: Evidence from geochronology and geochemistry of the Xigaze ophiolite, southern Tibet: *Lithos*, v. 172, p. 1–16, <https://doi.org/10.1016/j.lithos.2013.03.011>.
- Davies, H.J., and von Blanckenburg, F., 1995, Slab breakoff: A model of lithosphere detachment and its test in the magmatism and deformation of collisional orogens: *Earth and Planetary Science Letters*, v. 129, p. 85–102, [https://doi.org/10.1016/0012-821X\(94\)00237-S](https://doi.org/10.1016/0012-821X(94)00237-S).
- DeCelles, P.G., Ducea, M.N., Kapp, P., and Zandt, G., 2009, Cyclicity in Cordilleran orogenic systems: *Nature Geoscience*, v. 2, p. 251–257, <https://doi.org/10.1038/ngeo469>.
- DeCelles, P.G., Kapp, P., Gehrels, G.E., and Ding, L., 2014, Paleocene-Eocene foreland basin evolution in the Himalaya of southern Tibet and Nepal: Implications for the age of initial India-Asia collision: *Tectonics*, v. 33, p. 824–849, <https://doi.org/10.1002/2014TC003522>.
- DeCelles, P.G., Zandt, G., Beck, S.L., Currie, C.A., Ducea, M.N., Kapp, P., Gehrels, G.E., Carrapa, B., Quade, J., and Schoenbohm, L.M., 2015, Cyclical orogenic processes in the Cenozoic central Andes, in DeCelles, P.G., Ducea, M.N., Carrapa, B., and Kapp, P.A., eds., *Geodynamics of a Cordilleran Orogenic System: The Central Andes of Argentina and Northern Chile*: Geological Society of America Memoir, v. 212, p. 459–490, [https://doi.org/10.1130/2015.1212\(22\)](https://doi.org/10.1130/2015.1212(22)).
- Debon, F., Lefort, P., Dautel, D., Sonet, J., and Zimmermann, J.L., 1987, Granites of western Karakoram and northern Kohistan (Pakistan): A composite mid-Cretaceous to upper Cenozoic magmatism: *Lithos*, v. 20, p. 19–40, [https://doi.org/10.1016/0024-4937\(87\)90022-3](https://doi.org/10.1016/0024-4937(87)90022-3).
- de Sigoyer, J., Chavagnac, V., Blichert-Toft, J., Villa, I.M., Luais, B., Guillot, S., Cosca, M., and Mascle, G., 2000, Dating the Indian continental subduction and collisional thickening in the northwest Himalaya: Multichronology of the Tso Moriri eclogites: *Geology*, v. 28, p. 487–490, [https://doi.org/10.1130/0091-7613\(2000\)28<487:DTICSA>2.0.CO;2](https://doi.org/10.1130/0091-7613(2000)28<487:DTICSA>2.0.CO;2).
- de Sigoyer, J., Guillot, S., and Dick, P., 2004, Exhumation of the ultrahigh-pressure Tso Moriri unit in eastern Ladakh (NW Himalaya): A case study: *Tectonics*, v. 23, <https://doi.org/10.1029/2002TC001492>.
- Dewey, J.F., 1988, Extensional collapse of orogens: *Tectonics*, v. 7, p. 1123–1139, <https://doi.org/10.1029/TC007i006p01123>.
- Dewey, J.F., and Bird, J.M., 1970, Mountain belts and new global tectonics: *Journal of Geophysical Research*, v. 75, p. 2625–2647, <https://doi.org/10.1029/JB075i014p02625>.
- Dhuime, B., Wuestefeld, A., and Hawkesworth, C.J., 2015, Emergence of modern continental crust about 3 billion years ago: *Nature Geoscience*, v. 8, p. 552–555, <https://doi.org/10.1038/ngeo2466>.
- Ding, L., Kapp, P., and Wan, X.Q., 2005, Paleocene-Eocene record of ophiolite obduction and initial India-Asia collision, south central Tibet: *Tectonics*, v. 24, <https://doi.org/10.1029/2004TC001729>.
- Donaldson, D.G., Webb, A.A.G., Menold, C.A., Kylander-Clark, A.R.C., and Hacker, B.R., 2013, Petrochronology of Himalayan ultrahigh-pressure eclogite: *Geology*, v. 41, p. 835–838, <https://doi.org/10.1130/G33699.1>.
- Freeburn, R., Bouilhol, P., Maunder, B., Magni, V., and van Hunen, J., 2017, Numerical models of the magmatic processes induced by slab breakoff: *Earth and Planetary Science Letters*, v. 478, p. 203–213, <https://doi.org/10.1016/j.epsl.2017.09.008>.
- Frost, B.R., Barnes, C.G., Collins, W.J., Arculus, R.J., Ellis, D.J., and Frost, C.D., 2001, A geochemical classification for granitic rocks: *Journal of Petrology*, v. 42, p. 2033–2048, <https://doi.org/10.1093/petrology/42.11.2033>.
- Gao, P., Zheng, Y.F., and Zhao, Z.F., 2016, Experimental melts from crustal rocks: A lithochemical constraint on granite petrogenesis: *Lithos*, v. 266–267, p. 133–157, <https://doi.org/10.1016/j.lithos.2016.10.005>.
- Grove, T.L., Elkins-Tanton, L.T., Parman, S.W., Chatterjee, N., Muntener, O., and Gaetani, G.A., 2003, Fractional crystallization and mantle-melting controls on calc-alkaline differentiation trends: Contributions to Mineralogy and Petrology, v. 145, p. 515–533, <https://doi.org/10.1007/s00410-003-0448-z>.
- Guillot, S., Mahéo, G., de Sigoyer, J., Hattori, K.H., and Pêcher, A., 2008, Tethyan and Indian subduction viewed from the Himalayan high- to ultrahigh-pressure metamorphic rocks: *Tectonophysics*, v. 451, p. 225–241, <https://doi.org/10.1016/j.tecto.2007.11.059>.
- Guilmette, C., Hébert, R., Wang, C., and Villeneuve, M., 2009, Geochemistry and geochronology of the metamorphic sole underlying the Xigaze Ophiolite, Yarlung Zangbo Suture Zone, South Tibet: *Lithos*, v. 112, p. 149–162, <https://doi.org/10.1016/j.lithos.2009.05.027>.
- Guilmette, C., Hébert, R., Dostal, J., Indares, A., Ullrich, T., Bédard, É., and Wang, C., 2012, Discovery of a dismembered metamorphic sole in the Saga ophiolite mélange, South Tibet: Assessing an Early Cretaceous disruption of the Neo-Tethyan supra-subduction zone and consequences on basin closing: *Gondwana Research*, v. 22, p. 398–414, <https://doi.org/10.1016/j.jgr.2011.10.012>.
- Guo, Z., Wilson, M., and Liu, J., 2007, Post-collisional adakites in south Tibet: Products of partial melting of subduction-modified lower crust: *Lithos*, v. 96, p. 205–224, <https://doi.org/10.1016/j.lithos.2006.09.011>.
- Hébert, R., Bezard, R., Guilmette, C., Dostal, J., Wang, C.S., and Liu, Z.F., 2012, The Indus-Yarlung Zangbo ophiolites from Nanga Parbat to Namche Barwa syntaxes, southern Tibet: First synthesis of petrology, geochemistry, and geochronology with incidences on geodynamic reconstructions of Neo-Tethys: *Gondwana Research*, v. 22, p. 377–397, <https://doi.org/10.1016/j.jgr.2011.10.013>.
- Hermann, J., Zheng, Y.F., and Rubatto, D., 2013, Deep fluids in subducted continental crust: *Elements*, v. 9, p. 281–287, <https://doi.org/10.2113/gselements.9.4.281>.
- Hodges, K.V., 2000, Tectonics of the Himalaya and southern Tibet from two perspectives: *Geological Society of America Bulletin*, v. 112, p. 324–350, [https://doi.org/10.1130/0016-7606\(2000\)112<324:TOTHAS>2.0.CO;2](https://doi.org/10.1130/0016-7606(2000)112<324:TOTHAS>2.0.CO;2).
- Hou, Z., Yang, Z., Lu, Y., Kemp, A., Zheng, Y., Li, Q., Tang, J., Yang, Z., and Duan, L., 2015, A genetic linkage between subduction- and collision-related porphyry Cu deposits in continental collision zones: *Geology*, v. 43, p. 247–250, <https://doi.org/10.1130/G36362.1>.
- Hu, X.M., Garzanti, E., Moore, T., and Raffi, I., 2015, Direct stratigraphic dating of India-Asia collision onset at the Selandian (middle Paleocene, 59 ± 1 Ma): *Geology*, v. 43, p. 859–862, <https://doi.org/10.1130/G36872.1>.
- Hu, X., Garzanti, E., Wang, J., Huang, W., An, W., and Webb, A., 2016, The timing of India-Asia collision onset: Facts, theories, controversies: *Earth-Science Reviews*, v. 160, p. 264–299, <https://doi.org/10.1016/j.earscirev.2016.07.014>.
- Huangfu, P., Li, Z.-H., Gerya, T., Fan, W., Zhang, K.-J., Zhang, H., and Shi, Y., 2018, Multi-terrane structure controls the contrasting lithospheric evolution beneath the western and central-eastern Tibetan plateau: *Nature Communications*, v. 9, p. 3780, <https://doi.org/10.1038/s41467-018-06233-x>.
- Ji, W.Q., Wu, F.Y., Chung, S.L., Wang, X.C., Liu, C.Z., Li, Q.L., Liu, Z.C., Liu, X.C., and Wang, J.G., 2016, Eocene Neo-Tethyan slab breakoff constrained by 45 Ma oceanic island basalt-type magmatism in southern Tibet: *Geology*, v. 44, p. 283–286, <https://doi.org/10.1130/G37612.1>.
- Kaneko, Y., Katayama, I., Yamamoto, H., Misawa, K., Ishikawa, M., Rehman, H.U., Kausar, A.B., and Shiraiishi, K., 2003, Timing of Himalayan ultrahigh-pressure metamorphism: sinking rate and subduction angle of the Indian continental crust beneath Asia: *Journal of Metamorphic Geology*, v. 21, p. 589–599, <https://doi.org/10.1046/j.1525-1314.2003.00466.x>.
- Kapp, P., Decelles, P.G., Leier, A.L., Fabjanic, J.M., He, S., Pullen, A., Gehrels, G.E., and Ding, L., 2007, The Gangdese retroarc thrust belt revealed: *GSA Today*, v. 17, p. 4–9, <https://doi.org/10.1130/GSAT01707A.1>.
- Laskowski, A.K., Kapp, P., Vervoort, J.D., and Ding, L., 2016, High-pressure Tethyan Himalaya rocks along the India-Asia suture zone in southern Tibet: *Lithosphere*, v. 8, p. 574–582, <https://doi.org/10.1130/L544.1>.
- Laskowski, A.K., Kapp, P., Ding, L., Campbell, C., and Liu, X.H., 2017, Tectonic evolution of the Yarlung suture zone, Lopu Range region, southern Tibet: *Tectonics*, v. 36, p. 108–136, <https://doi.org/10.1002/2016TC004334>.
- Lee, H.Y., Chung, S.L., Ji, J., Qian, Q., Gallet, S., Lo, C.H., Lee, T.Y., and Zhang, Q., 2012, Geochemical and Sr-Nd isotopic constraints on the genesis of the Cenozoic Linzizong volcanic successions, southern Tibet: *Journal of Asian Earth Sciences*, v. 53, p. 96–114, <https://doi.org/10.1016/j.jseas.2011.08.019>.
- Leech, M.L., Singh, S., Jain, A.K., Klemperer, S.L., and Manickavasagam, R.M., 2005, The onset of India-Asia continental collision: Early, steep subduction required by the timing of UHP metamorphism in the western Himalaya: *Earth and Planetary Science Letters*, v. 234, p. 83–97, <https://doi.org/10.1016/j.epsl.2005.02.038>.
- Li, C., van der Hilst, R.D., Meltzer, A.S., and Engdahl, E.R., 2008, Subduction of the Indian lithosphere beneath the Tibetan Plateau and Burma: *Earth and Planetary Science Letters*, v. 274, p. 157–168, <https://doi.org/10.1016/j.epsl.2008.07.016>.
- Li, J.T., and Song, X.D., 2018, Tearing of Indian mantle lithosphere from high-resolution seismic images and its implications for lithosphere coupling in southern Tibet: *Proceedings of the National Academy of Sciences of the United States of America*, v. 115, p. 8296–8300, <https://doi.org/10.1073/pnas.1717258115>.
- Li, Y., Wang, C., Dai, J., Xu, G., Hou, Y., and Li, X., 2015, Propagation of the deformation and growth of the Tibetan-Himalayan orogen: A review: *Earth-Science Reviews*, v. 143, p. 36–61, <https://doi.org/10.1016/j.earscirev.2015.01.001>.
- Linnen, R.L., and Keppler, H., 2002, Melt composition control of Zr/Hf fractionation in magmatic processes: *Geochimica et Cosmochimica Acta*, v. 66, p. 3293–3301, [https://doi.org/10.1016/S0016-7037\(02\)00924-9](https://doi.org/10.1016/S0016-7037(02)00924-9).
- Liu, A.-L., Wang, Q., Zhu, D.-C., Zhao, Z.-D., Liu, S.-A., Wang, R., Dai, J.-G., Zheng, Y.-C., and Zhang, L.-L., 2018, Origin of the ca. 50 Ma Linzizong shoshonitic volcanic rocks in the eastern Gangdese arc, southern Tibet: *Lithos*, v. 304–307, p. 374–387, <https://doi.org/10.1016/j.lithos.2018.02.017>.
- Liu, G., and Einsele, G., 1994, Sedimentary history of the Tethyan basin in the Tibetan Himalayas: *Geologische Rundschau*, v. 83, p. 32–61, <https://doi.org/10.1007/BF00211893>.
- Mahéo, G., Blichert-Toft, J., Pin, C., Guillot, S., and Pêcher, A., 2009, Partial melting of mantle and crustal sources beneath South Karakoram, Pakistan: Implications for the Miocene geodynamic evolution of the India-Asia convergence zone: *Journal of Petrology*, v. 50, p. 427–449, <https://doi.org/10.1093/petrology/egp006>.
- Metcalfe, K., and Kapp, P., 2017, The Yarlung suture mélange, Lopu Range, southern Tibet: Provenance of sandstone blocks and transition from oceanic subduction to continental collision: *Gondwana Research*, v. 48, p. 15–33, <https://doi.org/10.1016/j.gr.2017.03.002>.
- Metcalfe, K., and Kapp, P., 2019, History of subduction erosion and accretion recorded in the Yarlung Suture Zone, southern Tibet, in Treloar, P.J., and Searle, M.P., eds., *Himalayan Tectonics: A Modern Synthesis*: Geological Society of London, Special Publications, v. 483, p. 517–554, <https://doi.org/10.1144/SP483.12>.
- Miller, C., Thoni, M., Frank, W., Schuster, R., Melcher, F., Meisel, T., and Zanetti, A., 2003, Geochemistry and tectonomagmatic affinity of the Yungbwa ophiolite, SW Tibet: *Lithos*, v. 66, no. 3–4, p. 155–172, [https://doi.org/10.1016/S0024-4937\(02\)00217-7](https://doi.org/10.1016/S0024-4937(02)00217-7).
- Mo, X., Niu, Y., Dong, G., Zhao, Z., Hou, Z., Zhou, S., and Ke, S., 2008, Contribution of syn-collisional felsic magmatism to continental crust growth: A case study of the Paleogene Linzizong volcanic Succession in southern Tibet: *Chemical Geology*, v. 250, p. 49–67, <https://doi.org/10.1016/j.chemgeo.2008.02.003>.

- Nábělek, J., Hetenyi, G., Vergne, J., Sapkota, S., Kaffle, B., Jiang, M., Su, H.P., Chen, J., Huang, B.S., and Hi, C.T., 2009, Underplating in the Himalaya-Tibet collision zone revealed by the Hi-CLIMB Experiment: *Science*, v. 325, p. 1371–1374, <https://doi.org/10.1126/science.1167719>.
- Najman, Y., Jenks, D., Godin, L., Boudagher-Fadel, M., Millar, I., Garzanti, E., Horstwood, M., and Bracciali, L., 2017, The Tethyan Himalayan detrital record shows that India–Asia terminal collision occurred by 54 Ma in the Western Himalaya: *Earth and Planetary Science Letters*, v. 459, p. 301–310, <https://doi.org/10.1016/j.epsl.2016.11.036>.
- Nelson, K.D., Zhao, W.J., Brown, L.D., Kuo, J., Che, J.K., Liu, X.W., Klempner, S.L., Makovskiy, Y., Meissner, R., Mechie, J., Kind, R., Wenzel, F., Ni, J., Nabelek, J., Chen, L.S., Tan, H.D., Wei, W.B., Jones, A.G., Booker, J., Unsworth, M., Kidd, W.S.F., Hauck, M., Alsdorf, D., Ross, A., Cogan, M., Wu, C.D., Sandvol, E., and Edwards, M., 1996, Partially molten middle crust beneath southern Tibet: Synthesis of project INDEPTH results: *Science*, v. 274, p. 1684–1688, <https://doi.org/10.1126/science.274.5293.1684>.
- Orme, D.A., and Laskowski, A.K., 2016, Basin analysis of the Albian-Santonian Xigaze Forearc, Lazi Region, South-Central Tibet: *Journal of Sedimentary Research*, v. 86, p. 894–913, <https://doi.org/10.2110/jsr.2016.59>.
- Orme, D.A., Carrapa, B., and Kapp, P., 2015, Sedimentology, provenance and geochronology of the upper Cretaceous–lower Eocene western Xigaze forearc basin, southern Tibet: *Basin Research*, v. 27, p. 387–411, <https://doi.org/10.1111/bre.12080>.
- Patriat, P., and Achahe, J., 1984, India-Eurasia collision chronology has implications for crustal shortening and driving mechanism of plates: *Nature*, v. 311, p. 615–621, <https://doi.org/10.1038/311615a0>.
- Pertermann, M., Hirschmann, M.M., Hametner, K., Günther, D., and Schmidt, M.W., 2004, Experimental determination of trace element partitioning between garnet and silica-rich liquid during anhydrous partial melting of MORB-like eclogite: *Geochemistry, Geophysics, Geosystems*, v. 5, no. 5, <https://doi.org/10.1029/2003GC000638>.
- Pichavant, M., and Macdonald, R., 2007, Crystallization of primitive basaltic magmas at crustal pressures and genesis of the calc-alkaline igneous suite: Experimental evidence from St Vincent. Lesser Antilles arc: Contributions to Mineralogy and Petrology, v. 154, p. 535–558, <https://doi.org/10.1007/s00410-007-0208-6>.
- Rapp, R.P., and Watson, E.B., 1995, Dehydration melting of metabasalt at 8–32 kbar: Implications for continental growth and crust-mantle recycling: *Journal of Petrology*, v. 36, p. 891–931, <https://doi.org/10.1093/ptrol/36.4.891>.
- Richards, A., Argles, T., Harris, N., Parrish, R., Ahmad, T., Darbyshire, F., and Draganits, E., 2005, Himalayan architecture constrained by isotopic tracers from clastic sediments: *Earth and Planetary Science Letters*, v. 236, p. 773–796, <https://doi.org/10.1016/j.epsl.2005.05.034>.
- Sanchez, V.L., Murphy, M.A., Robinson, A.C., Lapen, T.J., and Heizler, M.T., 2013, Tectonic evolution of the India–Asia suture zone since Middle Eocene time, Lopukangri area, south-central Tibet: *Journal of Asian Earth Sciences*, v. 62, p. 205–220, <https://doi.org/10.1016/j.jseaes.2012.09.004>.
- Searle, M.P., Windley, B.F., Coward, M.P., Cooper, D.J.W., Rex, A.J., Rex, D., Li, T.D., Xiao, X.C., Jan, M.Q., Thakur, V.C., and Kumar, S., 1987, The closing of Tethys and the tectonics of the Himalaya: *Geological Society of America Bulletin*, v. 98, p. 678–701, [https://doi.org/10.1130/0016-7606\(1987\)98<678:TCOTAT>2.0.CO;2](https://doi.org/10.1130/0016-7606(1987)98<678:TCOTAT>2.0.CO;2).
- Shi, D.N., Wu, Z.H., Klempner, S.L., Zhao, W.J., Xue, G.Q., and Su, H.P., 2015, Receiver function imaging of crustal suture, steep subduction, and mantle wedge in the eastern India-Tibet continental collision zone: *Earth and Planetary Science Letters*, v. 414, p. 6–15, <https://doi.org/10.1016/j.epsl.2014.12.055>.
- Shi, D.N., Zhao, W.J., Klempner, S.L., Wu, Z.H., Mechie, J., Shi, J.Y., Xue, G.Q., and Su, H.P., 2016, West-east transition from underplating to steep subduction in the India-Tibet collision zone revealed by receiver-function profiles: *Earth and Planetary Science Letters*, v. 452, p. 171–177, <https://doi.org/10.1016/j.epsl.2016.07.051>.
- Sisson, T.W., Ratajeski, K., Hankins, W.B., and Glazner, A.F., 2005, Voluminous granitic magmas from common basaltic sources: Contributions to Mineralogy and Petrology, v. 148, p. 635–661, <https://doi.org/10.1007/s00410-004-0632-9>.
- St-Onge, M.R., Rayner, N., Palin, R.M., Searle, M.P., and Waters, D.J., 2013, Integrated pressure–temperature–time constraints for the Tso Moriri dome (Northwest India): Implications for the burial and exhumation path of UHP units in the western Himalaya: *Journal of Metamorphic Geology*, v. 31, p. 469–504, <https://doi.org/10.1111/jmg.12030>.
- Sun, S.S., and McDonough, W.F., 1989, Chemical and isotopic systematics of oceanic basalts: Implications for mantle composition and processes: *Geological Society of London, Special Publications*, v. 42, p. 313–345, <https://doi.org/10.1144/GSL.SP.1989.042.01.19>.
- Tilmann, F., and Ni, J., and INDEPTH III Seismic Team, 2003, Seismic Imaging of the downwelling Indian lithosphere beneath central Tibet: *Science*, v. 300, p. 1424–1427, <https://doi.org/10.1126/science.1082777>.
- Ulmer, P., Kaegi, R., and Muntener, O., 2018, Experimentally derived intermediate to silica-rich arc magmas by fractional and equilibrium crystallization at 1.0 GPa: An evaluation of phase relationships, compositions, liquid lines of descent and oxygen fugacity: *Journal of Petrology*, v. 59, p. 11–58, <https://doi.org/10.1093/ptrol/egy017>.
- van de Zedde, D.M.A., and Wortel, M.J.R., 2001, Shallow slab detachment as a transient source of heat at midlithospheric depths: *Tectonics*, v. 20, p. 868–882, <https://doi.org/10.1029/2001TC001018>.
- Van der Voo, R., Spakman, W., and Bijwaard, H., 1999, Tethyan subducted slabs under India: *Earth and Planetary Science Letters*, v. 171, p. 7–20, [https://doi.org/10.1016/S0012-821X\(99\)00131-4](https://doi.org/10.1016/S0012-821X(99)00131-4).
- van Hinsbergen, D.J.J., Steinberger, B., Doubrovine, P.V., and Gassmüller, R., 2011, Acceleration and deceleration of India-Asia convergence since the Cretaceous: Roles of mantle plumes and continental collision: *Journal of Geophysical Research. Solid Earth*, v. 116, p. B06101.
- Wang, H.Q., Ding, L., Cai, F.L., Xu, Q., Li, S., Fu, J.J., Lai, Q.Z., Yue, Y.H., and Li, X., 2017a, Early Tertiary deformation of the Zhongba-Gyangze Thrust in central southern Tibet: *Gondwana Research*, v. 41, p. 235–248, <https://doi.org/10.1016/j.gr.2015.02.017>.
- Wang, H.Q., Ding, L., Kapp, P., Cai, F.-L., Clinkscales, C., Xu, Q., Yue, Y.H., Li, S., and Fan, S.Q., 2018, Earliest Cretaceous accretion of Neo-Tethys oceanic subduction along the Yarlung Zangbo Suture Zone, Sangsang area, southern Tibet: *Tectonophysics*, v. 744, p. 373–389, <https://doi.org/10.1016/j.tecto.2018.07.024>.
- Wang, J.G., Hu, X.M., Garzanti, E., An, W., and Liu, X.C., 2017b, The birth of the Xigaze forearc basin in southern Tibet: *Earth and Planetary Science Letters*, v. 465, p. 38–47, <https://doi.org/10.1016/j.epsl.2017.02.036>.
- Wang, R., Richards, J.P., Hou, Z.Q., An, F., and Creaser, R.A., 2015, Zircon U-Pb age and Sr-Nd-Hf-O isotope geochemistry of the Paleocene-Eocene igneous rocks in western Gangdese: Evidence for the timing of Neo-Tethyan slab breakoff: *Lithos*, v. 224, p. 179–194, <https://doi.org/10.1016/j.lithos.2015.03.003>.
- Wilke, F.D.H., O'Brien, P.J., Schmidt, A., and Ziemann, M.A., 2015, Subduction, peak and multi-stage exhumation metamorphism: Traces from one coesite-bearing eclogite, Tso Moran, western Himalaya: *Lithos*, v. 231, p. 77–91, <https://doi.org/10.1016/j.lithos.2015.06.007>.
- Wu, F.Y., Sun, D.Y., Li, H., Jahn, B.M., and Wilde, S., 2002, A-type granites in northeastern China: age and geochemical constraints on their petrogenesis: *Chemical Geology*, v. 187, p. 143–173, [https://doi.org/10.1016/S0009-2541\(02\)00018-9](https://doi.org/10.1016/S0009-2541(02)00018-9).
- Wu, F.Y., Ji, W.Q., Liu, C.Z., and Chung, S.L., 2010, Detrital zircon U-Pb and Hf isotopic data from the Xigaze fore-arc basin: Constraints on Transhimalayan magmatic evolution in southern Tibet: *Chemical Geology*, v. 271, p. 13–25, <https://doi.org/10.1016/j.chemgeo.2009.12.007>.
- Wu, F.Y., Ji, W.Q., Wang, J.G., Liu, C.Z., Chung, S.L., and Clift, P.D., 2014, Zircon U-Pb and Hf isotopic constraints on the onset time of India-Asia collision: *American Journal of Science*, v. 314, p. 548–579, <https://doi.org/10.2475/02.2014.04>.
- Xu, W.C., Zhang, H.F., Harris, N., Guo, L., Pan, F.B., and Wang, S., 2013, Geochronology and geochemistry of Mesoproterozoic granitoids in the Lhasa terrane, south Tibet: Implications for the early evolution of Lhasa terrane: *Precambrian Research*, v. 236, p. 46–58, <https://doi.org/10.1016/j.precamres.2013.07.016>.
- Yin, A., and Harrison, T.M., 2000, Geologic evolution of the Himalayan-Tibetan orogen: *Annual Review of Earth and Planetary Sciences*, v. 28, p. 211–280, <https://doi.org/10.1146/annurev.earth.28.1.211>.
- Zhang, H., Ji, W.Q., Zhang, S.H., Wang, J.G., and Wu, F.Y., 2019, Zircon U-Pb age and Hf isotope of intrusive rocks from the Yawa area in the west part of southern Lhasa terrane, Tibet: *Yanshi Xuebao*, v. 35, no. 2, p. 423–438.
- Zhang, S.Y., 2018, The characteristics and metallogenic potential of the Main-collisional intrusive rocks in the middle-western Gangdese region [M.A. dissertation]: Beijing, China University of Geosciences, p. 1–113.
- Zhang, Z., Xiang, H., Dong, X., Ding, H., and He, Z., 2015, Long-lived high-temperature granulite-facies metamorphism in the Eastern Himalayan orogen, south Tibet: *Lithos*, v. 212–215, p. 1–15, <https://doi.org/10.1016/j.lithos.2014.10.009>.
- Zhao, J., Yuan, X., Liu, H., Kumar, P., Pei, S., Kind, R., Zhang, Z., Teng, J., Ding, L., Gao, X., Xu, Q., and Wang, W., 2010, The boundary between the Indian and Asian tectonic plates below Tibet: *Proceedings of the National Academy of Sciences of the United States of America*, v. 107, p. 11229–11233, <https://doi.org/10.1073/pnas.1001921107>.
- Zheng, Y.-F., and Chen, Y.-X., 2016, Continental versus oceanic subduction zones: *National Science Review*, v. 3, p. 495–519, <https://doi.org/10.1093/nsr/nww049>.
- Zhou, X., Zheng, J.P., Xiong, Q., Yang, J.S., Wu, Y.B., Zhao, J.H., Griffin, W.L., and Dai, H.K., 2017, Early Mesozoic deep-crust reworking beneath the central Lhasa terrane (South Tibet): Evidence from intermediate gneiss xenoliths in granites: *Lithos*, v. 274, p. 225–239, <https://doi.org/10.1016/j.lithos.2016.12.035>.
- Zhu, B., Kidd, W.S.F., Rowley, D.B., Currie, B.S., and Shafique, N., 2005, Age of initiation of the India-Asia collision in the east-central Himalaya: *The Journal of Geology*, v. 113, p. 265–285, <https://doi.org/10.1086/428805>.
- Zhu, D.C., Zhao, Z.D., Niu, Y.L., Mo, X.X., Chung, S.L., Hou, Z.Q., Wang, L.Q., and Wu, F.Y., 2011, The Lhasa Terrane: Record of a microcontinent and its histories of drift and growth: *Earth and Planetary Science Letters*, v. 301, p. 241–255, <https://doi.org/10.1016/j.epsl.2010.11.005>.
- Zhu, D.-C., Zhao, Z.-D., Niu, Y., Dilek, Y., Hou, Z.-Q., and Mo, X.-X., 2013, The origin and pre-Cenozoic evolution of the Tibetan Plateau: *Gondwana Research*, v. 23, p. 1429–1454, <https://doi.org/10.1016/j.gr.2012.02.002>.
- Zhu, D.C., Wang, Q., Zhao, Z.D., Chung, S.L., Cawood, P.A., Niu, Y.L., Liu, S.A., Wu, F.Y., and Mo, X.X., 2015, Magmatic record of India-Asia collision: *Scientific Reports*, v. 5, no. 14289, <https://doi.org/10.1038/srep14289>.
- Zhu, D.-C., Wang, Q., Chung, S.-L., Cawood, P.A., and Zhao, Z.-D., 2019, Gangdese magmatism in southern Tibet and India-Asia convergence since 120 Ma, in Treloar, P.J., and Searle, M.P., eds., *Himalayan Tectonics: A Modern Synthesis*: Geological Society, London, Special Publications, v. 483, p. 583–604, <https://doi.org/10.1144/SP483.14>.

SCIENCE EDITOR: WENJIAO XIAO  
ASSOCIATE EDITOR: HAIJIANG ZHANG

MANUSCRIPT RECEIVED 20 SEPTEMBER 2019  
REVISED MANUSCRIPT RECEIVED 20 FEBRUARY 2020  
MANUSCRIPT ACCEPTED 31 JULY 2020

Printed in the USA